AD-A150 827 NON-STEADY COMBUSTION OF COMPOSITE SOLID PROPELLANTS 1/1
(U) JET PROPULSION LAB PASADENA CA N S COHEN ET AL.
MAY 84 JPL-D-1602 AFOSR-TR-85-0103 AFOSR-ISSA-83-00052
UNCLASSIFIED F/G 19/1 NL

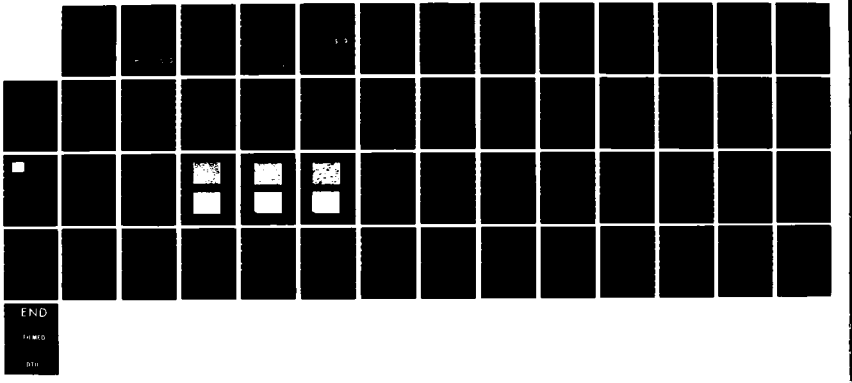

END
FILMED
DTIC

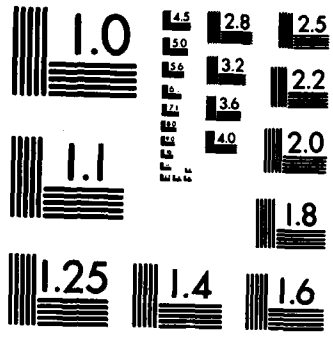

MICROCOPY RESOLUTION TEST CHART
NATIONAL BUREAU OF STANDARDS-1963-A

AFOSR-TR- 85-0103

JPL D-1602

3

Non-Steady Combustion of Composite Solid Propellants

Final Report

N.S. Cohen
L.D. Strand

May 1984

Prepared for
U.S. Air Force Office of Scientific Research
Through an agreement with
National Aeronautics and Space Administration
by

JPL
Jet Propulsion Laboratory
California Institute of Technology
Pasadena, California

UNCLASSIFIED

SECURITY CLASSIFICATION OF THIS PAGE (When Data Entered)

REPORT DOCUMENTATION PAGE		READ INSTRUCTIONS BEFORE COMPLETING FORM
1. REPORT NUMBER AFOSR-TR- 85-0108	2. GOVT ACCESSION NO. A150827	3. RECIPIENT'S CATALOG NUMBER
4. TITLE (and Subtitle) NON-STEADY COMBUSTION OF COMPOSITE SOLID PROPELLANTS		5. TYPE OF REPORT & PERIOD COVERED FINAL 1 Oct. 1980 - 31 March 1984
		6. PERFORMING ORG. REPORT NUMBER
7. AUTHOR(s) N S Cohen L D Strand		8. CONTRACT OR GRANT NUMBER(s) AFOSR-ISSA-83-00052
9. PERFORMING ORGANIZATION NAME AND ADDRESS JET PROPULSION LABORATORY CALIFORNIA INSTITUTE OF TECHNOLOGY PASADENA, CA 91109		10. PROGRAM ELEMENT, PROJECT, TASK AREA & WORK UNIT NUMBERS 61102F 2308/A1
11. CONTROLLING OFFICE NAME AND ADDRESS AIR FORCE OFFICE OF SCIENTIFIC RESEARCH/NA BOLLING AFB DC 20332-6600		12. REPORT DATE May 1984
		13. NUMBER OF PAGES 51
14. MONITORING AGENCY NAME & ADDRESS(if different from Controlling Office)		15. SECURITY CLASS. (of this report) Unclassified
		15a. DECLASSIFICATION/DOWNGRADING SCHEDULE

16. DISTRIBUTION STATEMENT (of this Report)

Approved for public release: Distribution unlimited

17. DISTRIBUTION STATEMENT (of the abstract entered in Block 20, if different from Report)

18. SUPPLEMENTARY NOTES

19. KEY WORDS (Continue on reverse side if necessary and identify by block number)

SOLID PROPELLANT COMBUSTION MODELING
COMBUSTION INSTABILITY

20. ABSTRACT (Continue on reverse side if necessary and identify by block number)

Analytical models were developed for the linearized pressure-coupled and velocity-coupled combustion response functions of composite propellants. The theory is that compositional fluctuations occur in the course of composite propellant burning, that these fluctuations originate from the inherent heterogeneity of the propellant microstructure, and that they will contribute to the nonsteady combustion under oscillating pressure (and velocity) conditions. Properties of the response to compositional fluctuations were →

DD FORM 1 JAN 73 1473 EDITION OF 1 NOV 65 IS OBSOLETE

UNCLASSIFIED

SECURITY CLASSIFICATION OF THIS PAGE (When Data Entered)

Block 20. Abstract (continued)

determined and compared with responses to pressure and velocity fluctuations in series of parametric studies. The response to compositional fluctuations was found to be a relatively strong response. Each response tended to increase with increasing AP particle size and pressure, and with decreasing mean cross-flow velocity.

A series of experiments was carried out with three propellants to determine whether or not certain features of the microstructure could be measured and correlated with response function behavior. Frequency components in the microstructure were measured and correlated with particle-size distribution. Frequency components were also measured in dynamic burning experiments carried out at constant pressure, but these were essentially independent of size distribution, and therefore not fully correlatable with size distribution. Response function measurements completed the series and indicated that the inherent microstructure is not the source of heterogeneous effects.

Additional tasks pertaining to nonlinear combustion response and high frequency combustion response were performed and are described in the text. A list of publications generated by or in the course of this program is presented.

It is concluded that the compositional response is an important mechanism to describe effects of heterogeneity, but that some process other than microstructure periodicities is needed for its proper implementation. Further study is recommended.

ACKNOWLEDGMENT OF GOVERNMENT RIGHTS
AND SPONSORSHIP

Research was sponsored by the Air Force Office of Scientific Research, Air Force Systems Command, USAF, under Contracts AFOSR ISSA-81-00019, 82-00030 and 83-00052, through an agreement with the National Aeronautics and Space Administration, NASA 7-100, Task Order RD-182, Amendments No. 132, 199 and 318. The United States Government is authorized to reproduce and distribute reprints for Governmental purposes notwithstanding any copyright notation thereon.

Accession For	
NTIS GRA&I	☑
DTIC TAB	☐
Unannounced	☐
Justification	
By	
Distribution/	
Availability Codes	
Dist	Avail and/or Special
A-1	

ABBREVIATIONS AND ACRONYMS

ABL	Alleghany Ballistics Laboratory
AFOSR	Air Force Office of Scientific Research
AFRPL	Air Force Rocket Propulsion Laboratory
AIAA	American Institute of Aeronautics and Astronautics
AP	ammonium perchlorate
CARDE	Canadian Armament Design and Experimental Establishment
EDAX	energy dispersive analysis of X-rays
HTPB	hydroxyl-terminated polybutadiene
JANNAF	Joint Army Navy NASA Air Force
JPL	Jet Propulsion Laboratory
PBAN	polybutadiene acrylonitrile
SEM	scanning electron microscope

NOMENCLATURE

a_o	=	mean speed of sound in the gas
d_j	=	a characteristic dimension in the propellant, possibly the particle size or a feature related to particle size
f_j	=	a characteristic frequency
i	=	$\sqrt{-1}$
K_n	=	ratio of propellant burn area to nozzle throat area
K_ρ	=	dependence of propellant density on α, $\left(\frac{\partial \ln \rho}{\partial \ln \alpha}\right)$
m_o	=	mean value of mass flux; m' = fluctuating component
n_p	=	pressure exponent, $\left(\frac{\partial \ln m}{\partial \ln p}\right)_{\alpha,\ T_i,\ u}$
n_u	=	velocity exponent, $\left(\frac{\partial \ln m}{\partial u/a_o}\right)_{\alpha,\ p,\ T_i}$
n_α	=	concentration exponent, $\left(\frac{\partial \ln m}{\partial \ln \alpha}\right)_{p,\ T_i,\ u}$
p_o	=	mean pressure; p' = fluctuating component
r_o	=	mean burning rate
R_p	=	pressure-coupled response function, $\left(\frac{m'/m_o}{p'/p_o}\right)$

R_c = classical component for a homogeneous medium, $\left(\frac{m'/m_o}{p'/p_o}\right)_{\alpha,\, u}$

R_α = heterogeneity component, at constant pressure, $\left(\frac{m'/m_o}{\alpha'/\alpha_o}\right)_{p,\, u}$

R_u = classical component of velocity-coupled response function for a homogeneous medium, $\left(\frac{m'/m_o}{u'/a_o}\right)_{\alpha,\, p}$

t = time

T_i = initial bulk temperature of the propellant

T_{w_o} = mean surface temperature

u_o = mean crossflow velocity; u' = fluctuating component

α_o = mean AP concentration; α' = fluctuating component

α_j = amplitude for the j^{th} component of heterogeneity

κ = thermal diffusivity

λ = a complex quantity dependent upon oscillatory frequency (Ref. 9)

ω_j = angular characteristic frequency

ρ = propellant density (note that K_ρ must be accounted for if it is desired to express n_α in terms of burning rate; n_α has been defined in terms of mass flux)

σ_p = temperature sensitivity, $\left(\frac{\partial \ln m}{\partial T_i}\right)_{\alpha, p, u}$

σ_T = $\left(\frac{\partial T_w}{\partial T_i}\right)_{\alpha, p, u}$

CONTENTS

Figures

Tables

SECTION 1

RESEARCH OBJECTIVES

1.1 OVERALL OBJECTIVE

The objective of this research program was to develop an understanding of oxidizer particle size effects on the non-steady combustion behavior of composite solid propellants. This understanding is expressed by the development of suitable analytical models to describe known or experimentally observed phenomena. A combination of theoretical and experimental tasks was performed toward the accomplishment of this objective. Results have been disseminated by technical presentations and publications, and through a variety of interchange functions with government laboratories and contractors. Demands of future propulsion systems and the viability of combustion tailoring through control of oxidizer particle size distribution make it imperative that the effects of size distribution be understood.

1.2 SPECIFIC OBJECTIVES FOR THIS PROGRAM

Particular attention has been given to the problem of combustion instability, which is promoted by the development of improved rocket motor capabilities for future missile systems. The specific objectives are listed as follows:

(1) Develop analytical models for the pressure-coupled and velocity-coupled combustion response functions, accounting for effects of ammonium perchlorate (AP) composite propellant heterogeneity.

(2) Develop experimental methods to characterize the heterogeneity of composite propellants and to complement the analytical models.

A literature survey on analytical response function models which account for effects of AP particle size (i.e., heterogeneity) was completed and published in the AIAA Journal (Ref.1). Following the survey, an analytical model was developed for the linear pressure-coupled response function (Ref. 2). This model accounts for the heterogeneity in two ways: effects of AP particle size on ballistics properties which enter into the response function theory; and compositional fluctuations at frequencies associated with characteristic dimensions of the heterogeneity. Publication of this work in the AIAA Journal is pending. The next step was the development of a model for the linear velocity-coupled response. The presence of crossflow and fluctuations in crossflow velocity are important aspects of combustion instability, and were added to the mechanisms contained in the pressure-coupled combustion response model. A paper based upon this work has been submitted to the AIAA for journal publication (Ref. 3). During the past year, the modeling was extended further to describe the non-linear combustion response. Non-linear instability is of importance to the Air Force, and much work on the gasdynamics aspects has been in progress in this field.

Three types of experiments have been conducted to characterize the heterogeneity of composite propellants and its effects on combustion behavior. The first experiment, which is non-destructive, is to perform energy dispersive analysis of X-rays (EDAX) scans of propellant samples under a scanning electron microscope (SEM). The data consist of fluctuations in chlorine intensities representative of local AP concentrations, and Fourier decomposition to determine frequency distributions of the fluctuations. The second experiment is use of the JPL microwave burner (Ref. 4) to measure dynamic burning rates in the absence of pressure fluctuations. A Fourier decomposition is made here, also, to determine frequency components. The third experiment is to use the microwave burner to measure the pressure-coupled combustion response as a function of the frequency of imposed pressure oscillations. Given the same set of propellants, it was desired to seek the consistent appearance of preferred frequencies and to relate observed frequencies to the heterogeneity of real propellants. These experiments were completed during the past year.

SECTION 2

ANALYTICAL MODEL DEVELOPMENTS

2.1 PRESSURE-COUPLED RESPONSE FUNCTION

A new analytical model was developed for the linear pressure-coupled combustion response function. The new feature of this model is that it contains a mechanism by which the heterogeneity of composite propellants provides a direct contribution to the combustion driving. Details were published in an AIAA paper (see Ref. 2) and in a dissertation that was informally distributed to interested colleagues (Ref. 5). A summary is given as follows.

2.1.1 Mechanism

It is postulated that there are inherent periodicities in the composition of a well-mixed composite propellant, owing to the structure of oxidizer (AP) particles in the medium of binder. The motion of any planar surface, representing the burning front, through the propellant will evoke the periodicities at frequencies represented by[1]

$$f_j = r_o/d_j \tag{1}$$

The periodicities in composition imply periodicities in the properties of the propellant which determine the burning rate (e.g., flame temperature). Thus the "steady-state" burning rate, r_o, would exist only as a time average. It is assumed that the periodicities in composition (and thereby in affected properties) may be represented by

$$\alpha = \alpha_o + \sum_j \alpha_j e^{i\omega_j t} \tag{2}$$

Perturbations in α will contribute to the acoustic driving if they occur at the same frequency as imposed pressure oscillations. Then an overall combustion response can be defined as a total derivative

$$R_p = R_c + R_\alpha \frac{\alpha'/\alpha_o}{p'/p_o} \tag{3}$$

2.1.2 Response Function Model

A linearized perturbation analysis provides expressions for the response function components as follows

---

[1] Symbols are defined in the Nomenclature

$$\frac{R_c}{n_p} = \frac{1}{1 - \sigma_p(T_{w_o} - T_i)(1 - \frac{1}{\lambda}) + \sigma_T(\lambda - 1)} \qquad (4)$$

$$\frac{R_\alpha}{n_\alpha} = \frac{1 - \frac{K_p}{n_\alpha}\sigma_p(T_{w_o} - T_i)(1 - \frac{1}{\lambda})}{1 - \sigma_p(T_{w_o} - T_i)(1 - \frac{1}{\lambda}) + \sigma_T(\lambda - 1)} \qquad (5)$$

In the absence of data for the combustion parameters, a combustion model can be used to calculate them. The model used in this study was the Cohen and Strand model (Ref. 6).

The new combustion parameter appearing is n_α, which expresses the dependence of burning rate on AP concentration in a manner analogous to pressure exponent. Thus it is called the "concentration exponent." Model calculations and experimental data reveal that the concentration exponent generally takes on values from 1-2 orders of magnitude larger than the pressure exponent. Thus the combustion response to compositional fluctuations, or the heterogeneity component, can be the dominant source of acoustic driving.

2.1.3 Parametric Studies

Two sets of parametric studies were performed with the model. In one, effects of parameters contained within Eqs. (4) and (5) on Rc and R_α as functions of frequency were explored. Results are typified by Figure 2-1, which shows the effect of temperature sensitivity on the peakedness of the response function curves. The second study explored effects of AP concentration, particle size, and pressure on these parameters and thereby on the response function curves. The Cohen and Strand combustion model was incorporated to make these calculations.

One interesting result of these calculations was that the effects upon the Eqs. (4) and (5) parameters were somewhat compensatory, which served to limit extremes of variation in the response function behavior. For example, increases in σ_p (destabilizing) tended to go with decreases in T_{w_o} and increases in σ_T (stabilizing). Large variations were still encountered, but not as extreme as might otherwise have been.

Effects of AP concentration, particle size, and pressure were not fully systematic, reflecting the complexity of the process interactions. As a general trend, high peak values of the combustion response are promoted by coarse AP and high pressure. These conditions favor combustion control by the AP flame, which is less stable than the diffusion flame because it is kinetically limited and less energetic. Low peak values of the combustion response

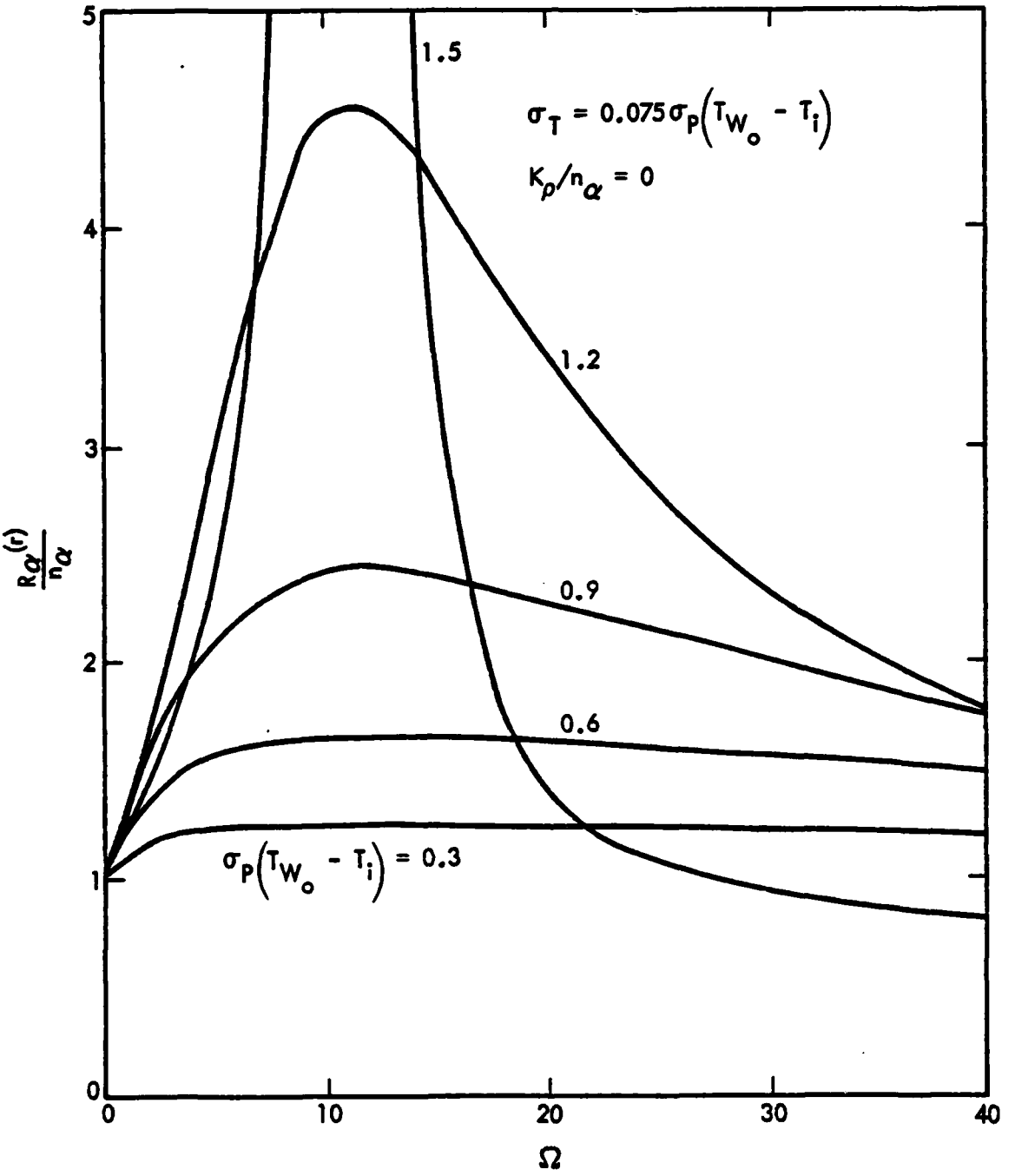

Figure 2-1. Effect of Temperature Sensitivity of Burn Rate on the Compositional Response

come about with fine intermediate-sized particles, within regimes of diffusion flame control. Peak response frequencies decrease with increasing particle size and decreasing pressure. Thus coarse AP tends to promote low frequency instability whereas fine AP tends to promote high frequency instability, but the peak responses with fine AP are lower. An example of these trends is given in Figure 2-2.

Another interesting result was the negative values of n_α computed to exist at AP concentrations on the oxidizer-rich side of stoichiometry. This would be highly stabilizing. That n_α can, in fact, be negative in this regime can be inferred by comparing the burning rate of pure AP with those of most propellants. Confirmation of the stability must await the processibility and test of propellants which are at least slightly oxidizer-rich (about 91% AP with HTPB binder). The growing state-of-the-art is approaching this capability, which is of interest for higher performance and burn rate in reduced-smoke propellants.

A final point is the provision for multi-peaked response function curves with this model. For a single-mode heterogeneity (one characteristic dimension, d_1), there will be a characteristic frequency associated with r_o/d_1 in addition to the classical thermal wave frequency associated with $r_o^{\ 2}/\kappa$. This idealized situation could therefore provide two distinct peaks. Real propellants would be expected to have a multiplicity of characteristic dimensions, such that the curve could exhibit multiple peaks unless the nature of the distribution causes them to diffuse into one another. For reasonable values of the combustion constants, the $r_o^{\ 2}/\kappa$ characteristic frequency cannot explain peaks at frequencies of the order of 10^2 Hz that are usually seen in data for composite propellants. Rather, it provides peaks at frequencies of the order of 10^3-10^4 Hz, which might be associated with the behavior of homogeneous propellants. Thus it would appear that the r_o/d_j frequencies are responsible for the behavior of composite propellants.

2.2 VELOCITY-COUPLED RESPONSE FUNCTION

The linearized combustion response to velocity perturbations was added to the foregoing model. Details were published in an AIAA paper (see Ref. 3). A summary is given as follows.

2.2.1 Mechanism

The basis for the theory is that velocity-coupling is the dynamic extension of steady-state erosive burning. This premise has been questioned, and research on dynamic combustion-flow interactions is in progress by colleagues. In the meantime, the modeling proceeded along this basis for information that it might uncover. In developing the combustion response model, an assumption was therefore made about the influence of the fluid mechanics merely to be able to state a boundary condition for the combustion analysis. As it turned out, useful information was uncovered.

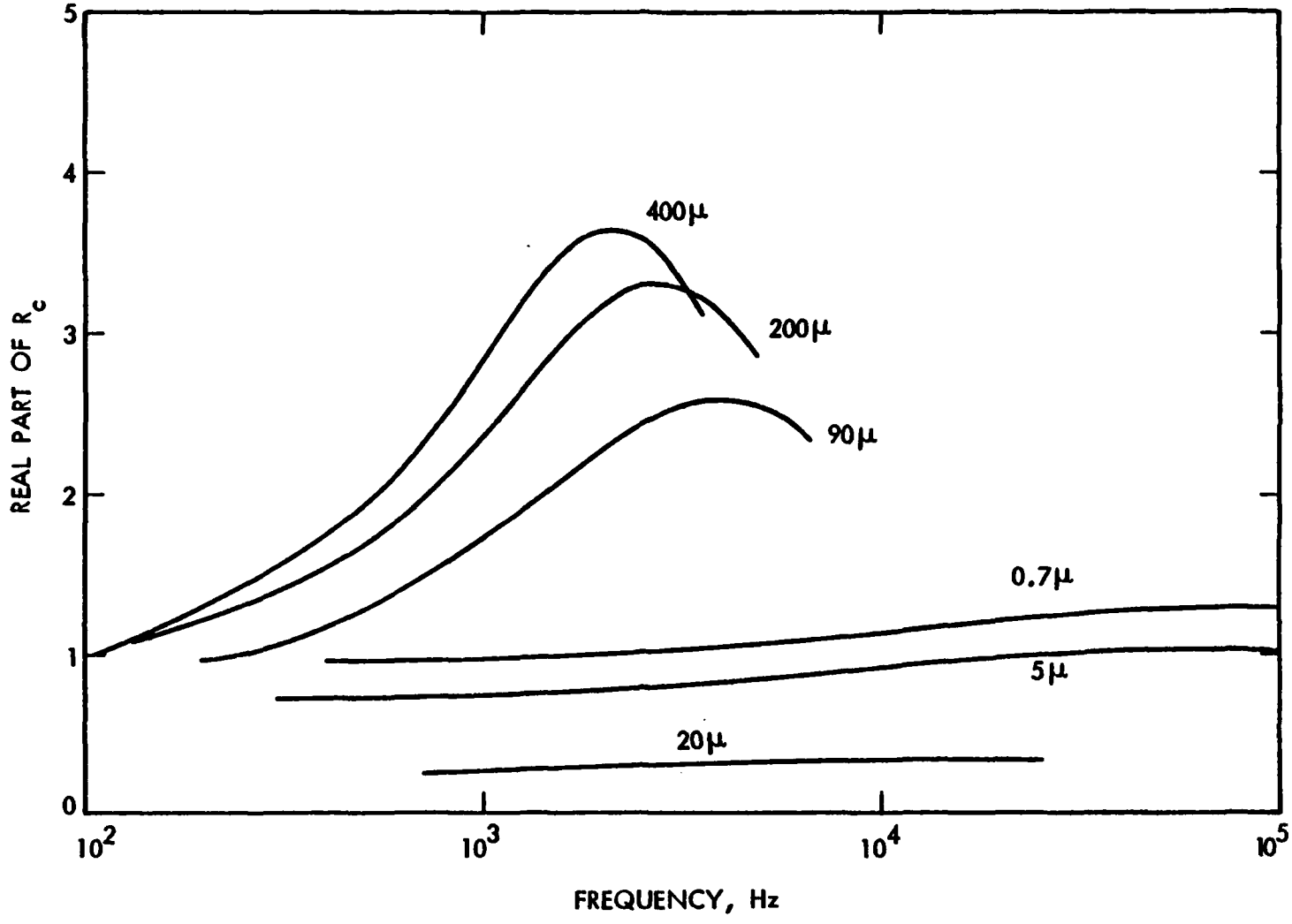

Figure 2-2. Effect of AP Particle Size on the R_c Combustion Response, 88% AP/HTPB, 6.8 MPa Pressure

2.2.2 Response Function Model

An erosive burning law of the form attributed to Saderholm (Ref. 7) was added to the energy equations of the Cohen and Strand combustion model. This law expressed the augmented heat feedback from the flames due to cross-flow. The physics embodied is no more and no less than that of conventional heat transfer theory with its semi-empiricisms. The resulting steady-state model was quantified by evaluation with the extensive erosive burning data of King (Ref. 8). Excellent comparisons inferred that particle-size effects on erosive burning arise only through their effects on r_o. A linearized pertur- bation analysis provides the following expressions for the velocity-coupled response function components

$$\frac{R_u}{n_u} = \text{Eq. (4)} \qquad (6)$$

$$\frac{R_u}{n_u} = \text{Eq. (5)} \qquad (7)$$

The analogous form of the equations is a fundamental aspect of combustion response theory (Ref. 9). The real parts of the equations are relevant to pressure-coupling, the imaginary parts are relevant to velocity-coupling.

2.2.3 Parametric Studies

Not much has been written about the "velocity exponent," n_u, as such in an analytical context. Model calculations and experimental data reveal that values of n_u are of comparable order to n_a, and therefore generally much larger than n_p. Consequently, the homogeneous response to pressure fluctuations is a relatively weak form of combustion response, and the heterogeneous component will not be as dominant for velocity-coupling as for pressure-coupling.

One set of parametric studies added the effects of mean flow, uo, on the controlling ballistics properties. Increasing uo tended to increase ro and np, and to decrease σp, n_a and n_u. A second set added the effects of u_o on the elements of the pressure-coupled response. Increasing u_o increases peak response frequencies, and tends to reduce those peak values of R_c and R_a which are largest in the absence of crossflow. Thus crossflow tends to stabilize the pressure-coupled response at lower frequencies and to destabilize it at higher frequencies. Effects of AP particle size were qualitatively the same as in the absence of crossflow.

The third set of parametric studies was conducted with respect to the elements of the velocity-coupled combustion response. As a general trend, high peak values of this combustion response are promoted by coarse AP, high pressure and low crossflow velocity. An example of the result is shown in Figure 2-3. Thus the potential for high values of the velocity-coupled response is coincident with that for the pressure-coupled response.

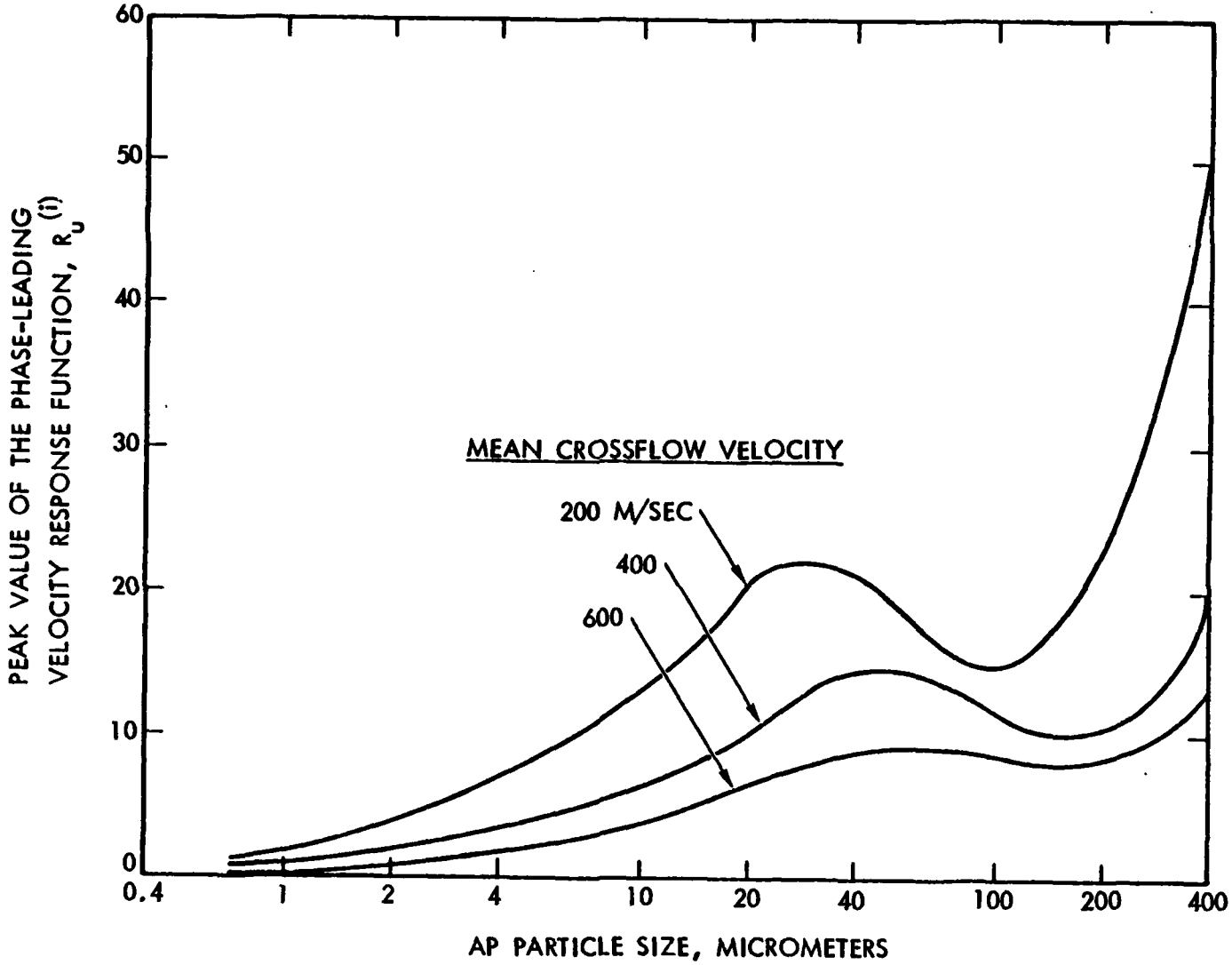

Figure 2-3. Effect of AP Particle Size and Mean Crossflow Speed on Peak Values of the Phase Leading (Positive) Velocity Response, 88% AP/HTPB, 13.6 MPa Pressure

One interesting result is the fact that a strong velocity-coupled response is promoted by low mean flow velocities, not high mean flow velocities. This, of course, requires that the low mean flow be at least above erosive threshold levels. The reason is that the effect of crossflow on the combustion diminishes with increasing velocity; in other words, n_u decreases with increasing u_o. What is important is the effect of the velocity perturbations, rather than velocity itself.

A second interesting result is that peak values of the velocity-coupled response will tend to be larger than those of the pressure-coupled response. This is mainly a consequence of the fact that n_u is larger than n_p.

A third interesting result is that multiple peaks in the pressure-coupled response will correspond to multiple zeroes in the velocity-coupled response.

All of the foregoing trends have at least circumstantial experimental confirmation in laboratory data and motor test experience. This does not of itself validate the theory, or the proposed mechanism for effects of heterogeneity, but it can be stated that some framework for interpretation and application to problems has been provided.

2.3 NONLINEAR COMBUSTION RESPONSE

2.3.1 Triggered Instability

Nonlinear combustion instability has been defined as an unstable response to a large disturbance under circumstances where the system is stable to small perturbations. Since the system is linearly stable, the large disturbance is said to "trigger" the instability. It is of practical interest because triggered instabilities have been encountered in ground test and flight experience; disturbances can arise in the operation of a rocket motor. Also, by simulating disturbances in testing, it is possible to develop a conservative design from the standpoint of stability.

There are several features of combustion instability which are nonlinear in nature. For example, even a linear instability will achieve a limiting pressure amplitude due to nonlinear effects. A linearized perturbation analysis will not be adequate to characterize these features. Either the perturbation analysis must include higher order terms, or the analysis must take the form of a direct numerical solution of the normal time-dependent equations. In any event, the triggering boundary is the feature of greatest interest.

The strongest element of current nonlinear analysis is the gasdynamics of the rocket motor chamber. A computer program providing an "exact" numerical solution of the conservation equations is available (Ref. 10). Several approximate higher order perturbation analyses are also available (Refs. 11-13). The weakest elements are the combustion model and the uncertainty of how triggering actually comes about. The foregoing referenced nonlinear analyses contain a very simple form of combustion model, which is inadequate to treat composite propellants.

The most extensive series of published experiments on the subject of triggering was carried out at the Canadian Armament Design and Experimental Establishment (CARDE) (Refs. 14-16). A triggering boundary was ascertained in terms of a critical pressure that could be associated with a critical motor K_n. Triggering was fostered by higher pressures. That work was reviewed as a part of this program. It was found that triggering could also be associated with a critical flow velocity in the port; triggering was fostered by a lower mean flow velocity. Another observation was that triggering was fostered by lower burning rate propellants. It is recalled that the model for linear velocity-coupling shows a stronger combustion response with increasing pressure, decreasing mean flow velocity and decreasing burn rate. This correlation of combustion model trends with motor experience, while not conclusive, was encouraging for the purpose of applying the model to the regime of nonlinear behavior.

2.3.2 Analytical Model

Analytical modeling work carried out during the past year was directed toward incorporating the Cohen and Strand combustion model, including effects of heterogeneity, into one of the nonlinear analysis frameworks. It was recognized that much needs to be learned regarding the nonsteady flow aspects, in particular the wall layer interactions near the propellant surface. But in the absence of better information, and pending research progress by colleagues, it was decided to proceed with this combustion aspect in order to achieve something better than currently available.

The framework selected was the exact nonlinear analysis computer program of the Air Force Rocket Propulsion Laboratory (AFRPL) (see Ref.10). A copy of the program listing was acquired and reviewed for needed modifications, interfacing and compatability considerations.

The AFRPL code provides a numerical integration of the heat conduction equation in a moving solid, which is the heart of any nonlinear time-dependent combustion model (Ref. 17). Unique features of the Cohen and Strand model involve the composite propellant heterogeneity and associated mechanism for combustion driving. These give rise to several problems in incorporating the model into the AFRPL code, which are discussed as follows.

First, the AFRPL code assumes a homogeneous propellant. The heterogeneity of composite propellants is built in by a function generator of the form of Eq. (2), which provides the fluctuating AP concentration at any instant of time in the course of burn. This is an input, and for this purpose there need not be a limit on the number of j components of the heterogeneity that can be included. However, a procedural problem is raised because the initial condition for the transient calculation is a precalculated "steady-state" equilibrium condition. With heterogeneity, there is really no steady-state because burning rate fluctuations will be calculated even at constant pressure. Therefore, there needs to be a heterogeneity start-up calculation prior to the imposition of a disturbance.

The second consideration arises from the boundary conditions of the transient heat conduction equation in the solid. There is no problem with the in-depth condition, which remains the same, but the new combustion model changes the description of the heat transfer as the boundary condition at the

propellant surface. If it were just a matter of being a different homogeneous combustion model, it could be incorporated in a straightforward manner as a subroutine replacing the existing model. What gives rise to problems is the capability of the new model to treat multimodal AP particle size distributions.

The present AFRPL code calculates a single surface temperature without regard to AP, binder or different AP particle sizes. Associated with this single surface temperature is a single, uniform description of the surface boundary condition. The code iterates for surface temperature consistent with the boundary condition, which results in a single instantaneous burning rate. On the other hand, the Cohen and Strand combustion model is capable of calculating 6 surface temperatures and regression rates conforming to 6 surface boundary conditions: AP and binder for each of the three particle sizes. The propellant burning rate is an aggregate of these contributions. There are several ways of resolving this major difference in the models.

It turns out that the transient heat conduction calculation is the most time-consuming step in the AFRPL code, and it is done at each of several axial locations along the length of the motor. An interpolative procedure is used to determine instantaneous burning rates at additional axial locations. It was considered that multiplying this procedure by a factor of 6 to accommodate the full heterogeneity capability would be prohibitive, and unwarranted in view of the model uncertainties. The approach adopted was a compromise between the mechanistic features of the heterogeneity and the practicality of a single surface temperature calculation.

In the new procedure, the boundary condition is established from a weighted average of the six (three AP and three binder) component contributions. These are calculated for the prevailing conditions by the combustion model as a subroutine. Use of the model as a subroutine is enabled by the quasi-steady gas assumption, which is valid for the low-intermediate frequencies of interest for the nonlinear instabilities treated by the AFRPL code. Thus the six surface temperatures, regression rates and heat transfers are effectively reduced to one for mating with the calculations presently in the AFRPL code. At the same time, however, the fluctuations in the individual components at their characteristic frequencies will still be felt through their influence on the average values. Since the combustion model is limited to three particle sizes, the heterogeneity (j) is effectively limited to three groupings.

In the course of iterations, discrepancies between trial and calculated values are handled by making pro-rata adjustments to the component contributions for the new trials. This procedure addresses the reverse problem of converting a calculated average to new component trials, to the extent that the calculated average differs from the previous trial average. Because of these complexities, it is not possible to verify analytically that the nonlinear combustion response reduces to the linear response in the limit of small perturbations. Such verification would have to be performed numerically.

Progress was limited to structuring the code for the foregoing modifications and additions, but the actual computer programming was not completed. Because of the uncertainties (about the microstructure periodicity mechanism) in the model, emphasis was instead placed on the series of diagnostic experiments and analysis of data to be discussed in Section 3.

2.4 HIGH FREQUENCY COMBUSTION RESPONSE

An additional task for FY 1982 was a limited study of the high frequency combustion response of minimum smoke (nitramine/energetic binder) propellants. This class of propellants is notorious for its propensity to exhibit high frequency transverse mode instability. As a first step, the scope of applicability of the quasi-steady gas assumption was carefully evaluated. This limitation on the theory is often talked about, but one does not see numbers reported. It was determined that the assumption is valid to a frequency of 16 KHz for a high energy propellant at a boost pressure (ca. 17 MPa), and therefore valid for many conditions of interest. Given that, the second step was to examine the viability of the classical two-parameter combustion response theory for minimum smoke propellants. There is evidence that minimum smoke propellants behave as homogeneous propellants. Using generally accepted values for the combustion constants of minimum smoke propellants, it was found that satisfactory response function curves could be generated. Therefore, it appears that the classical theory is worthy of further use in the study of minimum smoke propellants.

Finally, some work began on a reformulation of the Tien theory (Ref. 18), which relaxes the quasi-steady gas assumption. That theory is suspect because it predicts a pervasive regime of a negative response which is contrary to experience. Indeed, Flandro, in using the theory, found it necessary to force positive responses at frequencies where motors were unstable (Ref. 19). Progress did not go beyond setting up the analysis, as reported last year, because of other priorities and information that colleagues were addressing this problem under other Air Force programs. However, the results cited above furnish a basis for a future AIAA Journal technical note.

SECTION 3

EXPERIMENTS TO CHARACTERIZE HETEROGENEITY EFFECTS

3.1 SCANNING ELECTRON MICROSCOPE STUDIES

3.1.1 Experimental Method

A nondestructive method was developed for the study of the heterogeneity of composite propellants. The method makes use of the energy dispersive analysis of X-rays (EDAX) technique in association with a scanning electron microscope (SEM). It is based upon the fact that AP has chlorine atoms and binder does not. Therefore, an EDAX image of a magnified propellant sample, using a chlorine return, will show AP particles as white and interstitial binder as black. This permits AP and binder to be clearly identified, and also enables the image to be used for certain quantitative analyses. The information of interest here is the compositional fluctuations inherent in the propellant microstructure due to the heterogeneity.

The image is stored on a photographic negative for analysis by means of a microdensitometer. The magnification selected depends upon the range of particle sizes encountered. It should be large enough to resolve the smaller particles, yet small enough to acquire a statistical representation of the larger particles. For very wide distribution propellants, 2 magnifications would be recommended and results could be superposed. The image-processing microdensitometer/Fourier analyzer divides the negative into incremental areas consisting of the length and approximately 0.2% of the width. For each area or scan line, an integrated average gray level is measured. This average gray level is proportional to the AP concentration along that scan line. Fluctuations in the average gray level are measured as the microdensitometer proceeds from scan line to scan line. Results are presented in the form of average gray level versus distance and, by Fourier decomposition, the dimensional frequency components of the fluctuations in the average gray level.

Initial work was performed with the ideal geometry shown in Figure 3-1a. This geometry represents a unimodal propellant consisting of spherical particles in a closely-packed hexagonal array. The fluctuations in the average gray level are shown in Figure 3-1b, and the frequency components are shown in Figure 3-1c. The regularity in the fluctuations is as would be expected. Note that there is a multiplicity of frequency components. The first six, which are the largest, can be associated with the particle diameter, particle radius, and four dimensions which are characteristic of the interstitial spacings. Thus it is erroneous to equate preferred frequency behavior to the particle size alone, even for an ideal geometry.

Several windows were investigated for the Fourier transformations: the triangular (Parzen), hyperbolic cosine (Hanning) and rectangular windows. Excellent agreement was achieved in every case where all three windows were compared. Therefore, there is every confidence that the frequency distributions acquired are good data. However, edge effects in the samples distorted the power spectral levels toward the lower frequencies, which prevented the

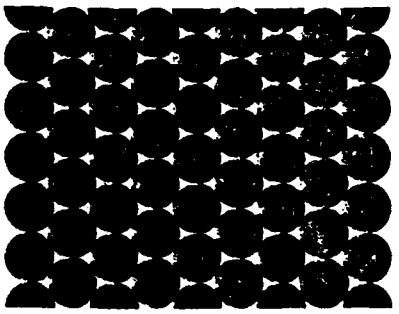

Figure 3-1(a). Idealized Structure of Unimodal Composite Propellant

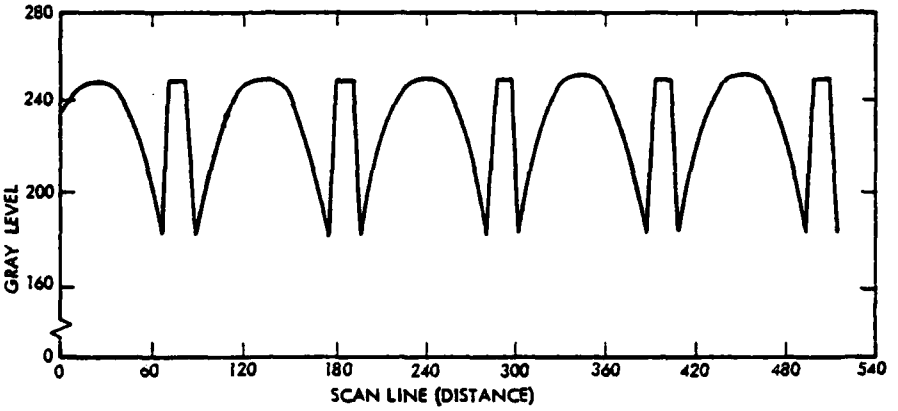

Figure 3-1(b). Fluctuations in Average Grey Level Along Scan Lines

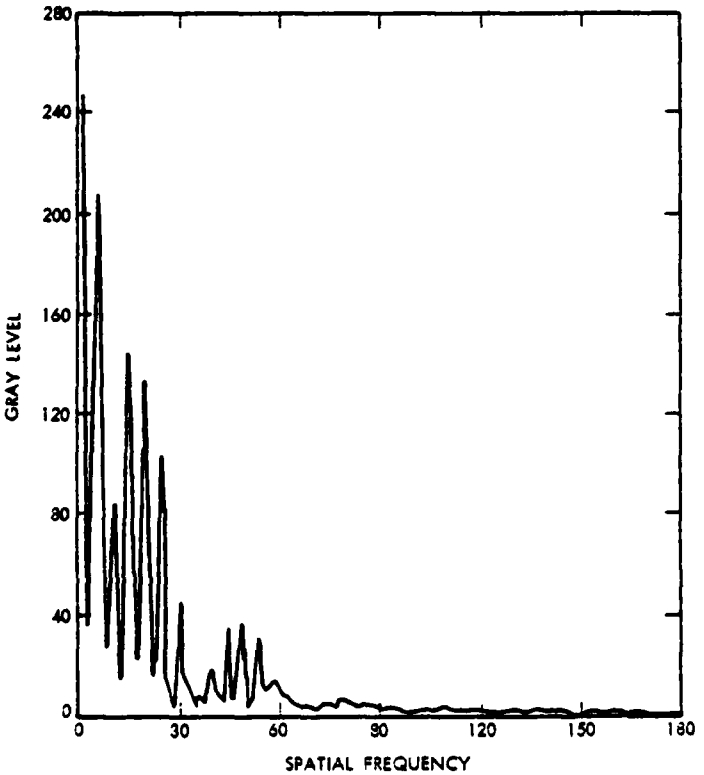

Figure 3-1(c) Frequency Components of Scan Line Grey Level Averages

reliable acquisition of amplitude data. Various techniques were attempted to minimize the edge effects, but did not turn out successful. Consequently, the amplitude data were limited to rough estimates of compositional fluctuations from the raw data. For example, Figure 3-1b represents a 35% total fluctuation in "AP concentration" for the packed bed of unimodal spheres. This agrees well with theoretical geometric calculations (variation from 72% AP to 95% AP, or a ratio of 1.32). Figure 3-1c illustrates the power distortion to lower frequencies.

Repeatability of the heterogeneity was evaluated by altering the image orientation of a sample and by selecting samples from different locations in the propellant carton. Samples were extracted by cutting propellant which had been cooled. Through practice, it was found that cooling the propellant prevented smearing of the cut surface by binder, and it was possible to achieve cut surfaces without pulling away surface AP particles. The samples were examined under the SEM prior to data acquisition to assure that the cutting did not introduce distortions.

A by-product of this research that was noted almost immediately was its applicability to the subjects of propellant processing and mechanical properties. Real propellants are not packed beds of unimodal spheres. They contain distributions of particle sizes and shapes, and it could be observed that they do not always appear to be uniform on the local microscopic scale. Clusters of AP and pockets of binder were sometimes noted with interest. A related subject would be the dispersion of solid catalysts and the migration of liquid catalysts or other additives in propellants. The EDAX/SEM technique can be useful for many purposes.

3.1.2 Propellants

Three propellants were specially processed to conduct the series of experiments. The solids loading (AP content) was restricted to 75% by weight because it was desired that two of the propellants be monomodal. It is close to an upper limit concentration to process a monomodal fine AP propellant, and suffices to avoid settling with a monomodal coarse AP propellant. The binder was hydroxyl-terminated polybutadiene (HTPB).

The fine particle-size distribution contained sizes ranging from 1 μm to 45 μm, with a mass mean of 11 $\pm$ 3 μm. This is referred to as "10 μm AP." It was attempted to narrow the distribution of the coarse size by using the size fraction that passed through a 212 μm, but not a 180 μm sieve. Deagglomeration of the material was apparently not entirely successful, because some smaller size material, down to 40 μm in size, remained. The mass mean value was 196 + 16 μm, and it is referred to as "200 μm AP."

The coarse AP propellant was designated LS-87, and had a burn rate of 0.51 cm/sec at 3.5 MPa. The pressure of 3.5 MPa was the standard pressure for combustion tests. The fine AP propellant was designated LS-88, and had a burn rate of 0.53 cm/sec. The third propellant was a bimodal 1/1 mixture of the fine and coarse size distributions. It was designated LS-89, and had a burn rate of 0.43 cm/sec. Curiously, the bimodal propellant had the lowest burn rate and there was not a significant difference between the coarse AP and fine AP propellant burn rates.

3.1.3 Results

Representative SEM photographs and their EDAX chlorine images for the three propellants are shown in Figures 3-2 through 3-4. The magnifications (indicated on the figure captions) were selected to resolve the smaller particles while acquiring a statistical representation of the larger particles, as stated earlier. The corresponding microdensitometer and Fourier analysis results for the Figure 3-2 through 3-4 SEM/EDAX maps are given in Figures 3-5 through 3-7. The verticle scales do not correspond to Figures 3-1b and 3-1c, so the propellants can be compared to the ideal spheres only qualitatively from these figures. As would be expected, the propellants did not show fluctuations or spectra as strongly as did the spheres, so enhancement was necessary. The propellants did show some regularities in the microdensitometer fluctuations, such that spectra could be derived, but clearly the regularity in the spheres is much more vivid. Figures 3-5 through 3-7 are typical of the quality of the data; there are examples of better data, and some not as good.

Characteristic dimensions extracted from the data are summarized in Table 3-1. These display all of the peaks that could be resolved. The strongest peaks are denoted by asterisks; as noted earlier, the strength was skewed toward the lower frequencies (coarser dimensions). Of interest is the repeatability of occurrence of these peaks over all of the samples for each propellant. This is presented in the Table footnote. The repeatability is observed to average about 50%, which means that on the average each of the indicated dimensions appeared in half of the samples. Thus these dimensions do have significance. The repeatability may not be equivalent to the idealized spheres, but it is more than a haphazard result.

The characteristic dimensions are displayed in Table 3-1 in such a way that the differences between the coarse and fine propellants are pointed out, and to be able to see how the coarse and fine propellants are reflected in the bimodal propellant. It appears that the characteristic dimensions can be associated with respective ranges of particle sizes in the propellants, and that the bimodal propellant does for the most part reflect its coarse and fine components.

A curious aspect of the results is that finer dimensions were not detected. In the case of the coarse propellant, interstitial spaces would be expected to be smaller than 45 μm, and the image was capable of resolving dimensions as small as 6 μm. In the case of the fine propellant, the size distribution goes down to 1 μm, and the image was capable of resolving it. Yet these finer dimensions did not produce detectable peaks. It is possible that they were simply too weak to appear, being of a more random nature and located at the high frequency portions of the repective spectra. Thus it would seem that the particle sizes are more significant than the interstitial spacings, but in the case of the fine AP propellant roughly 30% by weight of the particle sizes did not produce spectra.

Unfortunately, a magnitude of fluctuation could not be assigned to each characteristic dimension. Instead, what was done was to extract an RMS value of the fluctuations in AP concentration from the raw data for each of the propellants. Results are summarized in Table 3-2.

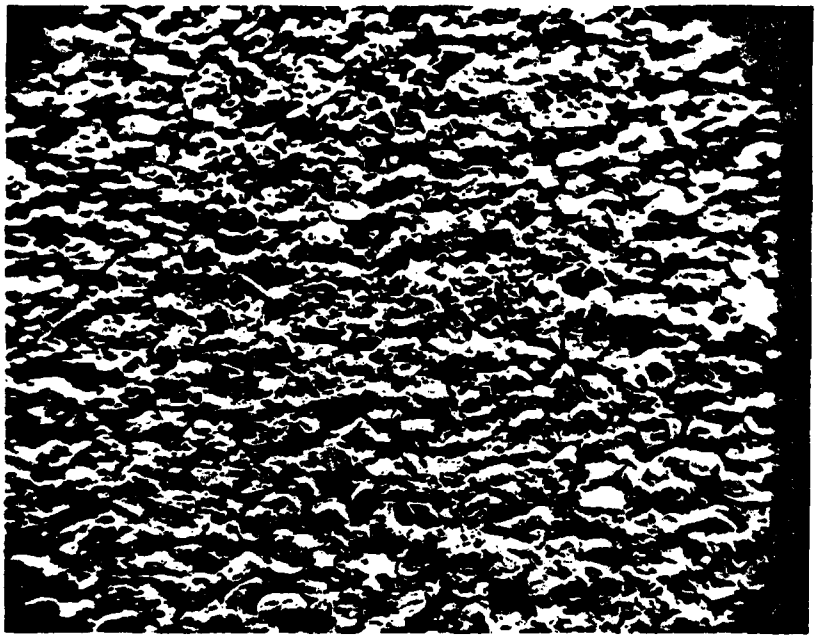

Figure 3-2(a). SEM Photograph of LS-87 (Coarse AP) Propellant Surface, 24X

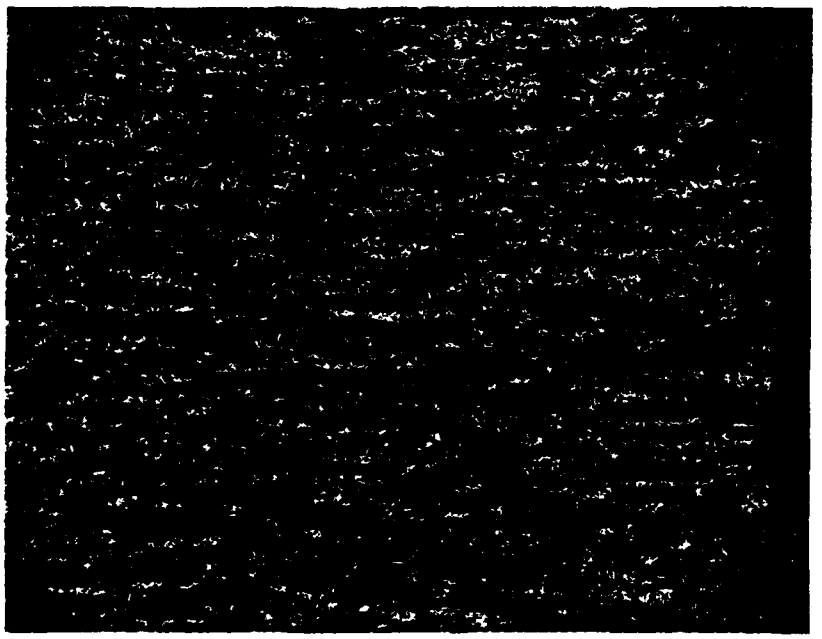

Figure 3-2(b). EDAX Chlorine Map of Figure 3-2(a) Surface

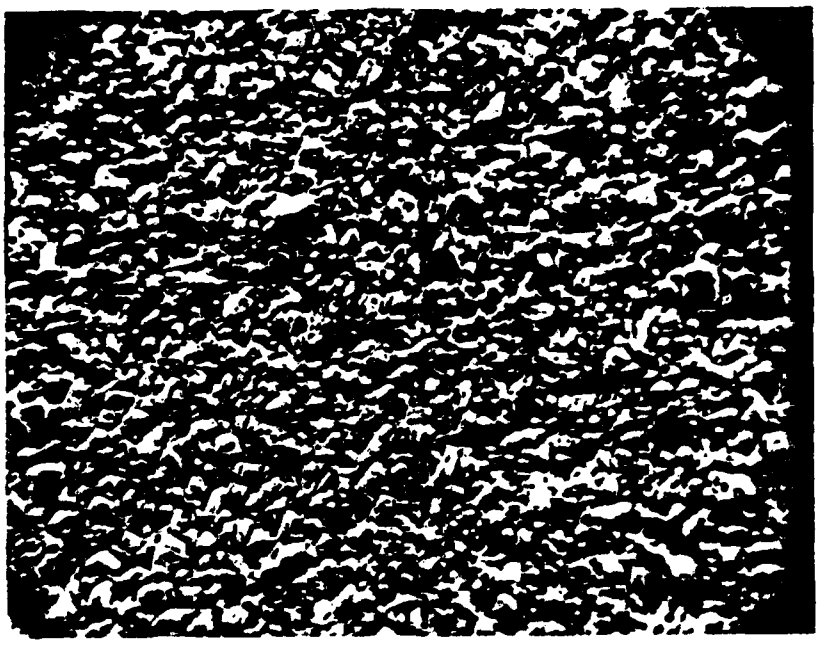

Figure 3-3(a). SEM Photograph of LS-88 (Fine AP) Propellant Surface, 130X

Figure 3-3(b). EDAX Chlorine Map of Figure 3-3(a) Surface

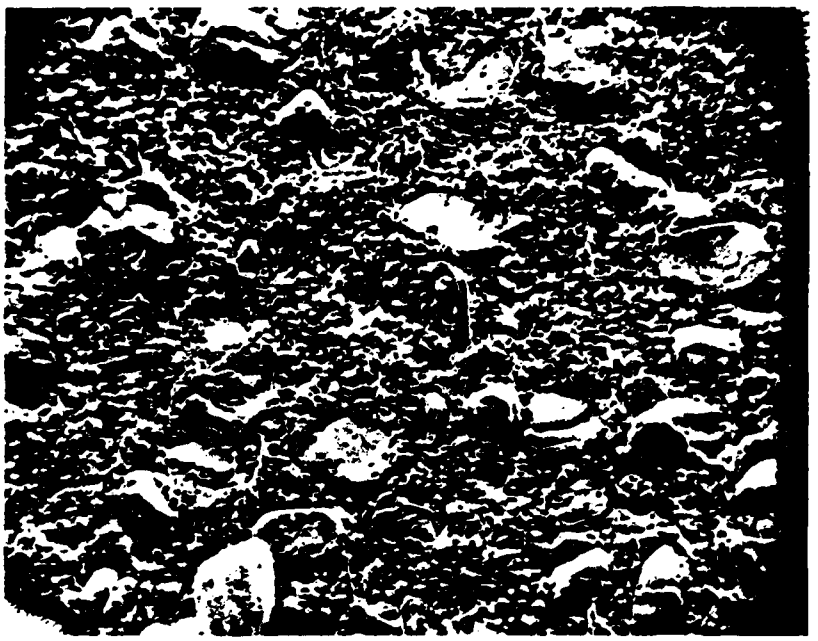

Figure 3-4(a). SEM Photograph of LS-89 (Bimodal AP) Propellant Surface, 60X

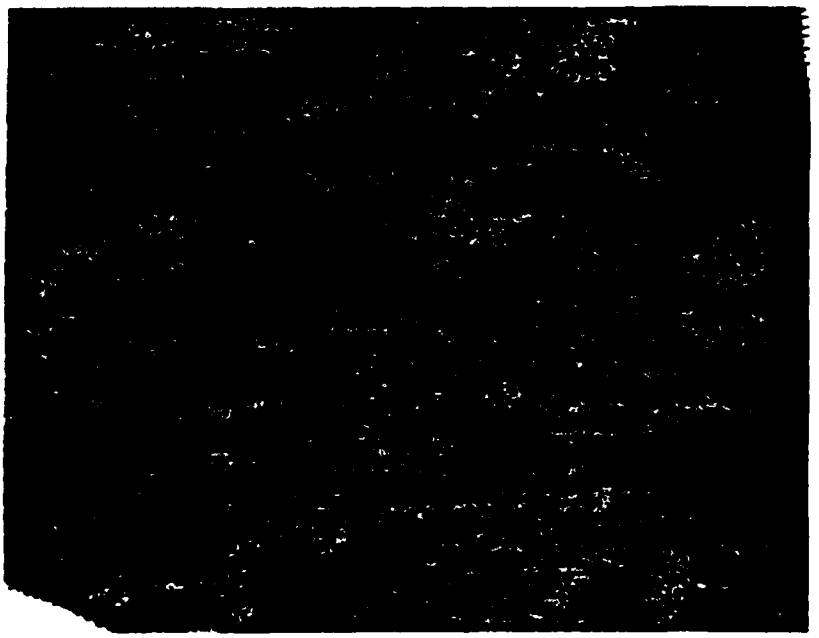

Figure 3-4(b). EDAX Chlorine Map of Figure 3-4(a) Surface

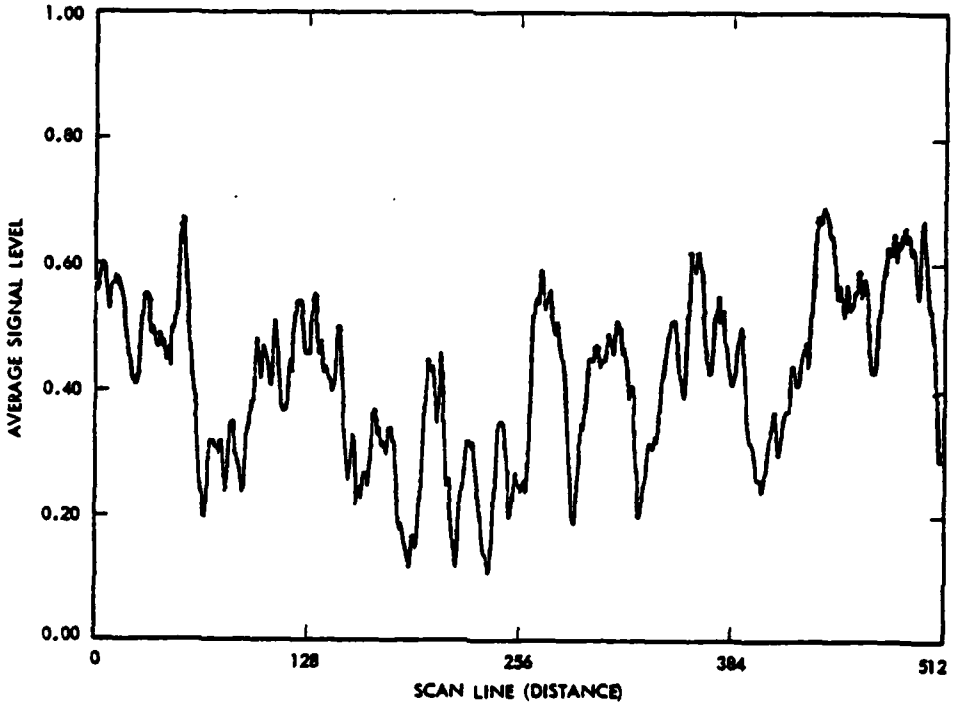

Figure 3-5(a). Analysis of Figure 3-2(b), EDAX Chlorine Map of LS-87 Propellant - (a) Fluctuations in Average Signal Level Along Scan Lines

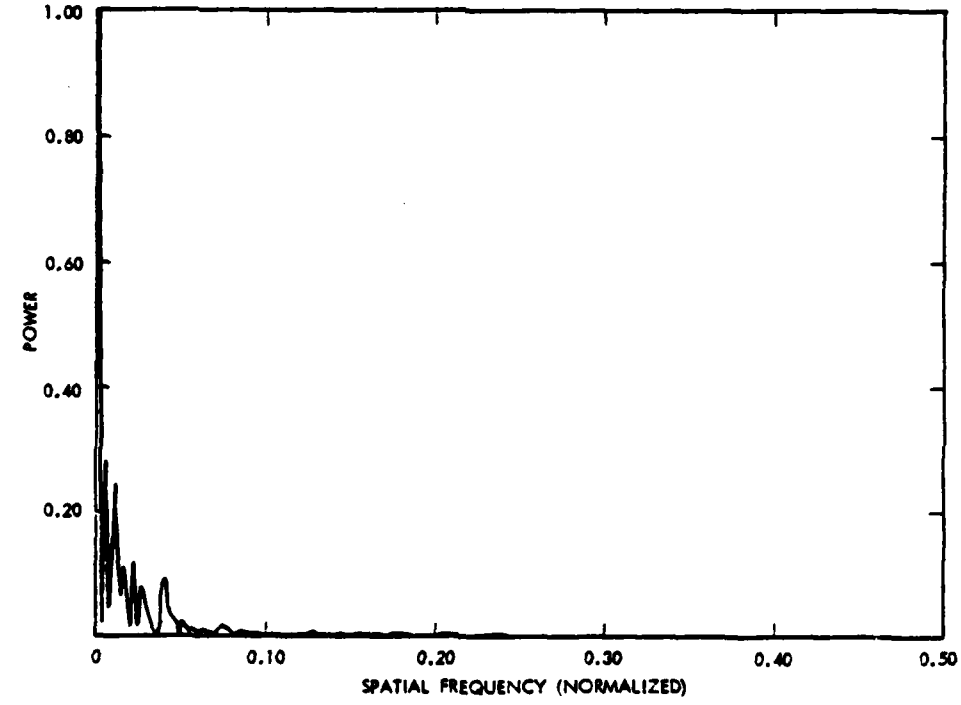

Figure 3-5(b). Analysis of Figure 3-2(b), EDAX Chlorine Map of LS-87 Propellant - (b) Frequency Components of Scan Line Signal Level Averages

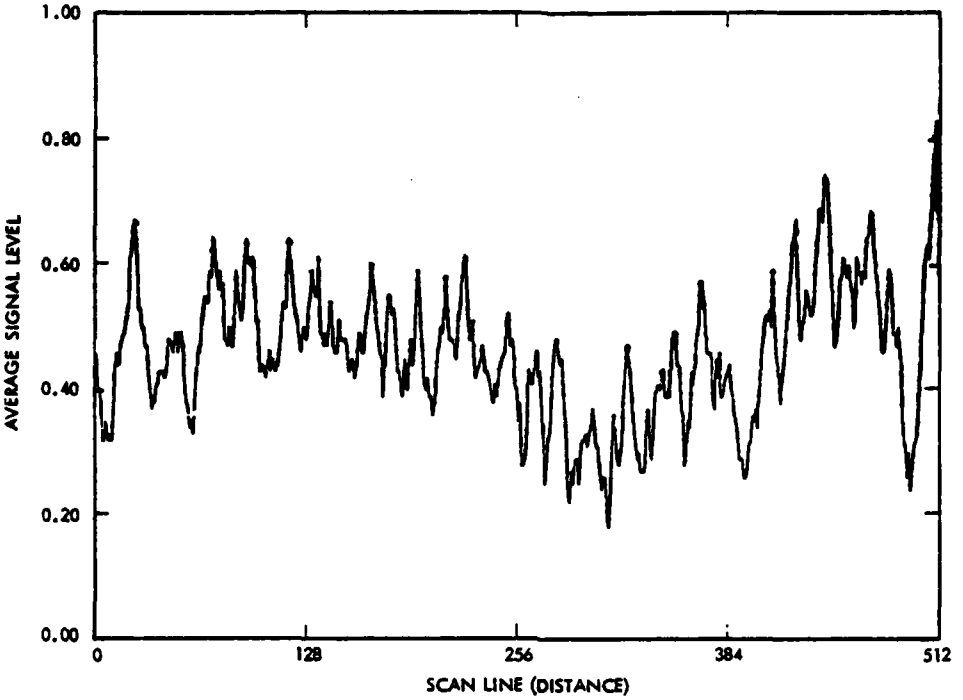

Figure 3-6(a). Analysis of Figure 3-3(b), EDAX Chlorine Map of LS-88 Propellant - (a) Fluctuations in Average Signal Level Along Scan Lines

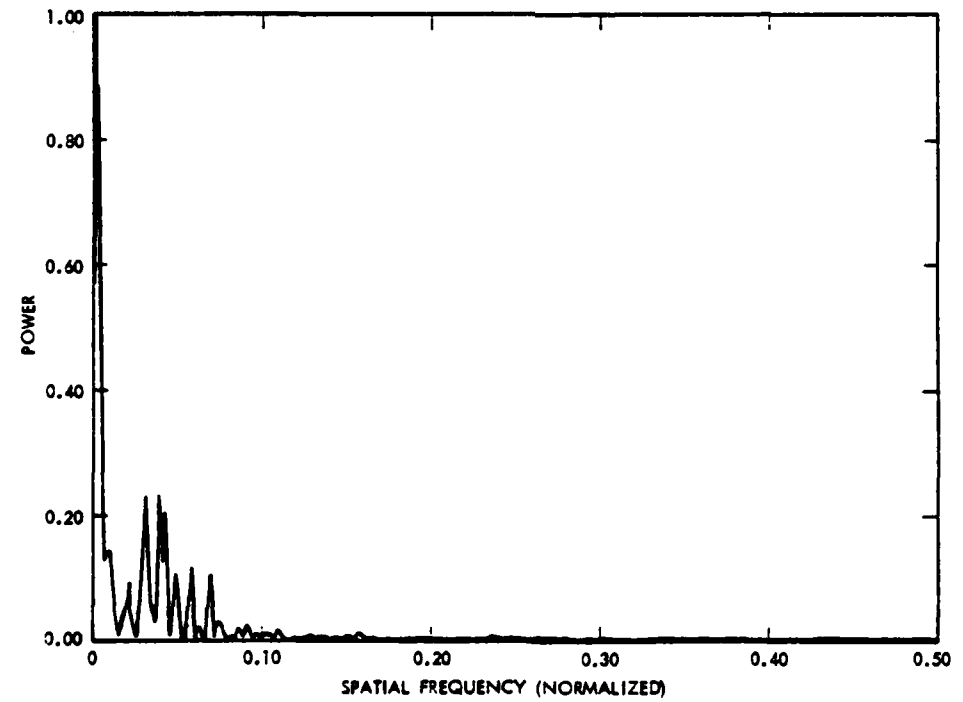

Figure 3-6(b). Analysis of Figure 3-3(b), EDAX Chlorine Map of LS-88 Propellant - (b) Frequency Components of Scan Line Signal Level Averages

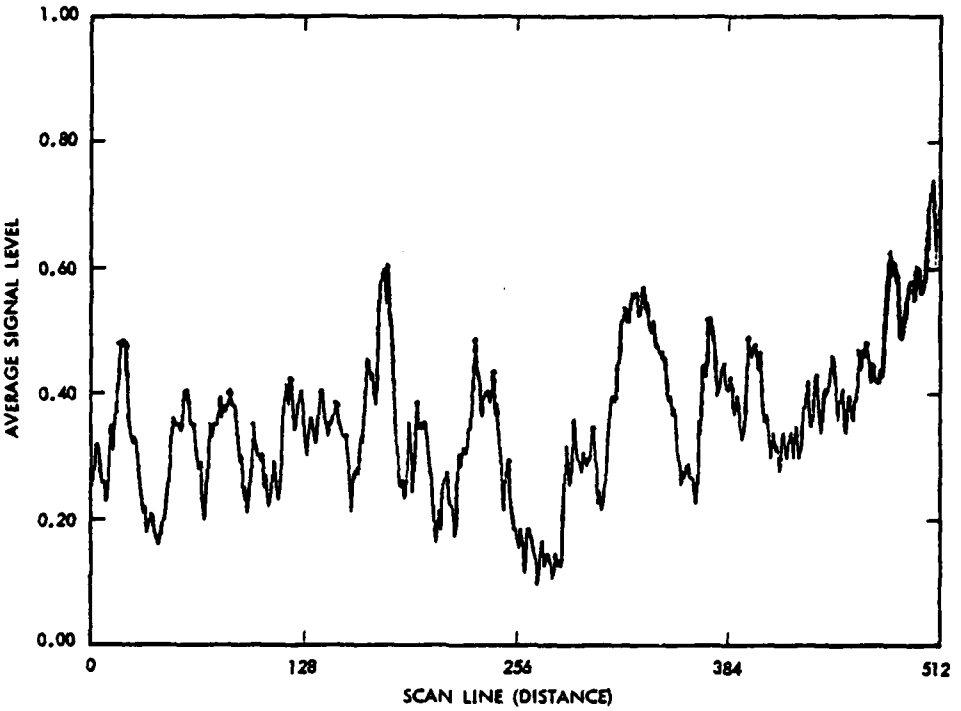

Figure 3-7(a). Analysis of Figure 3-4(b), EDAX Chlorine Map of LS-89 Propellant - (a) Fluctuations in Average Signal Level Along Scan Lines

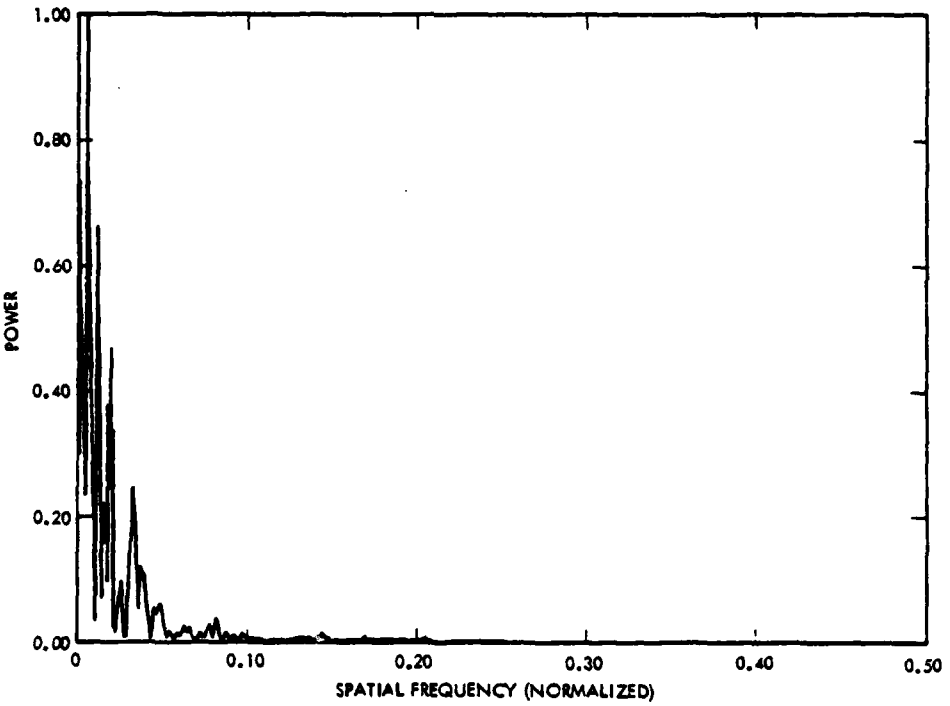

Figure 3-7(b). Analysis of Figure 3-4(b), EDAX Chlorine Map of LS-89 Propellant - (b) Frequency Components of Scan Line Signal Level Averages

Table 3-1. Characteristic Dimensions Corresponding to Frequency Components of Compositional Fluctuations, EDAX Data

Coarse AP[a] LS-87		Fine AP[b] LS-88		Bimodal AP[c] LS-89	
398 µm	*			381 µm	*
322	*				
302	*				
245	*				
215	*			223	*
185	*			189	*
171					
153	*			148	*
138					
127				127	*
109				111	
96					
89					
84				86	*
75				78	*
65		66 µm	*	68	*
58				60	*
55				54	
52		51			
45		43	*	43	*
		39	*	37	
		35		33	
		32	*	29	
		27	*	27	
		22	*	22	
		19	*	19	
		15		15	
		12		12	
		11		10	
		9			
		8		8	

a - 47% repeat occurrences
b - 55% repeat occurrences
c - 56% repeat occurrences

* denotes strong peaks

Table 3-2. RMS Fluctuations in AP Concentration, from EDAX Data

LS-87 (196 μm)	75.0 ± 6.6% AP
LS-88 (11 μm)	75.0 ± 3.6%
LS-89 (196/11 = 1/1)	75.0 ± 3.6%
A-13 (61 μm)	76.0 ± 4.1%

Included are data for A-13, the JANNAF standard propellant, which contains 61 μm (mass mean, monomodal) AP in PBAN binder. The A-13 data were acquired in the course of developing the technique last year. The magnitudes of the fluctuations are notable, though much smaller than for the ideal spheres. They are of roughly comparable magnitude among the various propellants, and appear to increase with increasing particle size for the monomodal propellants. Thus coarser AP propellants tend to exhibit stronger fluctuations, a point that might be relevant to the propensity for driving instability. The average fluctuation in the bimodal propellant appears to be dominated by the behavior of the fine component, perhaps because on a numerical basis there is so much more of the fines.

3.2 DYNAMIC BURNING AT CONSTANT PRESSURE

3.2.1 Experimental Method

Burning rate fluctuations at constant pressure were measured in the Jet Propulsion Laboratory (JPL) microwave burner apparatus, which has been described in Ref. 4. Ordinarily, this device is used to measure combustion response under conditions of imposed oscillatory pressures. With pressure held constant, fluctuations in burn rate could be attributed to heterogeneities and correlated with the EDAX data. Combustion response under oscillatory pressures was measured in the next phase of this work.

As might be expected, the dynamic burning at constant pressure did not produce frequency components having strong signal strengths. Considerable time and effort was devoted to improving the signal/noise ratio of the data. A portion of a typical test record is shown in Figure 3-8. The dynamic burning rate is proportional to the time differential of the Doppler phase shift of the microwave test signal. The spectra was scanned and averaged over the time interval for each 360^{o} total shift in phase of the reflected microwave signal, yielding several scans of data per test. Two or three tests were analyzed for each propellant, allowing the repeatability of the spectra to be evaluated. The testing was conducted at a pressure of 3.5 MPa.

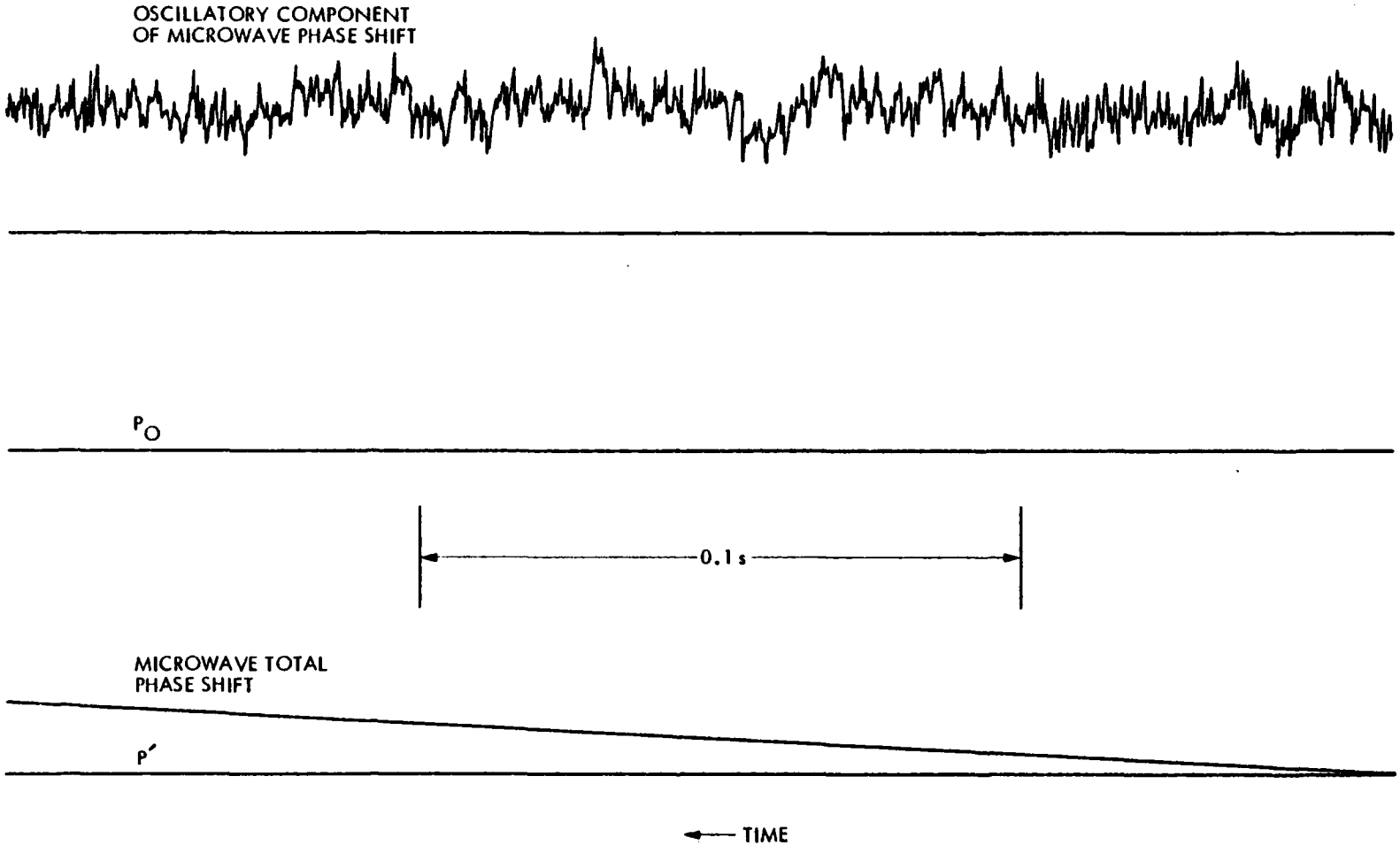

Figure 3-8. Portion of Test Record of Dynamic Burning Rate Data at Constant Pressure of 3.5 MPa - LS-87 Propellant

3.2.2 Results

Frequency components of dynamic burning at constant pressure are typified by the spectrum shown in Figure 3-9, an analysis of one time-interval portion of an LS-87 propellant test. Best results were achieved by plotting the log of the signal/background-noise ratio as a method to normalize out the noise. It is observed that there is a broad band of frequency components. Unfortunately, the lowest frequency components become masked by the D.C., having the effect of again distorting amplitudes to lower frequencies.

Characteristic dimensions associated with the frequency components are listed for the three propellants in Table 3-3. Repeat occurrences of the frequencies was quite good, averaging about 80%. However, expected differences between the three propellants did not appear. Unlike the EDAX results, the three propellants produced about the same dynamic burning spectra. Furthermore, the range of characteristic dimensions encompassed finer sizes here than in the EDAX data. Possible reasons may be the masking of coarser dimensions associable with the coarse and bimodal propellants by D.C., and the ability of the dynamic burning to resolve higher frequencies than could the EDAX. Another possibility, perhaps supported by the sameness and repeatability, is that something else in the system is responsible for these frequencies. Nevertheless, comparing the dynamic burning and EDAX results provides the list of characteristic dimensions common to both experiments in Table 3-4.

A rough estimate of the magnitude of the burning rate fluctuations was made from the raw data. The fluctuations were of the order of 0.1 cm/sec. Since the measured compositional fluctuations were about 4% AP, the combustion response to heterogeneity (R_λ) can be calculated to be about 4. This is a very reasonable result in the light of theoretical model calculations.

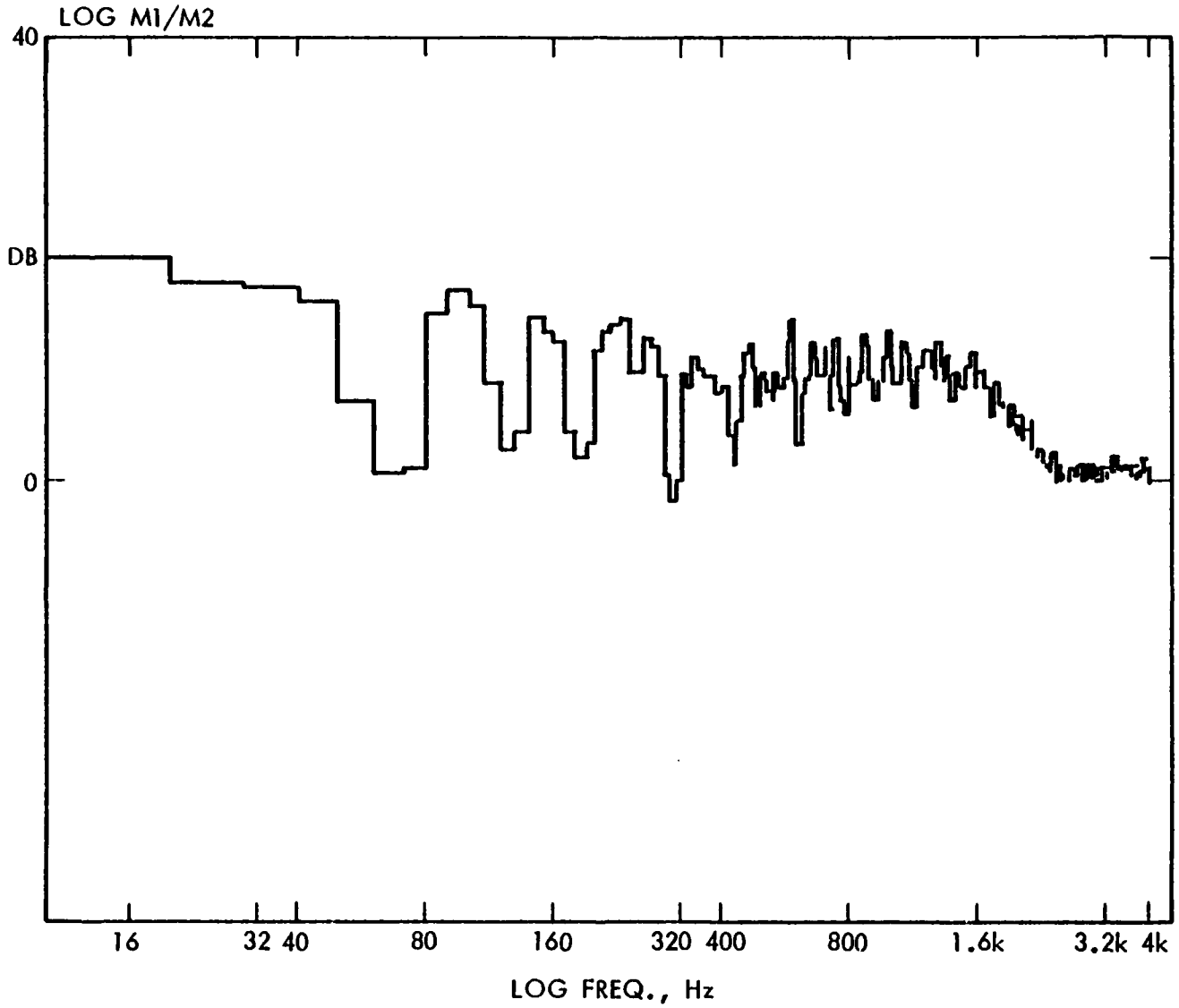

Figure 3-9. Frequency Components of Dynamic Burning Rate of LS-87 Propellant at Constant Pressure of 3.5 MPa

Table 3-3. Characteristic Dimensions Corresponding to Frequency Components of Burn Rate Fluctuations

Coarse AP[a] LS-87		Fine AP[b] LS-88		Bimodal AP[c] LS-89	
		54 μm*		51 μm*	
45 μm*					
		38	*	35	*
		26	*		
19	*	19	*	19	*
16		16	*	16	*
		15			
		13		13	
12		12			
		11	*	11	*
		10		10	
9	*	9	*	9	*
8		8		8	
7	*	7		7	*
6	*	6	*	6	*
5	*	5		5	
4		4	*	4	*
3		3	*	3	
2		2		2	*
1		1		1	

a - 77% repeat occurrences
b - 74% repeat occurrences
c - 89% repeat occurrences

* denotes strong peaks

Table 3-4. Characteristic Dimensions Common to EDAX and Dynamic Burning Experiments

Coarse AP LS-87	Fine AP LS-88	Bimodal AP LS-89
	51-54 μm	51-54 μm
45 μm		
	38-39	35-37
	26-27	
	19	19
	15	15-16
	12	12-13
	11	10-11
	9	9-10
	8	8

3.3 COMBUSTION RESPONSE MEASUREMENTS

3.3.1 Experimental Method

The microwave burner (Ref. 4) was used to measure the combustion response to pressure fluctuations over a range of frequencies from 20 Hz to 1200 Hz. The standard mean pressure was 3.5 MPa. Narrow frequency increments were selected to discern peaks in the real part of the combustion response. An important feature of the microwave technique is the ability to measure the phase of the response, which facilitates locating the peaks in the real part through the zeroes in the imaginary part.

An example of the raw dynamic burning data under conditions of oscillatory pressure is given in Figure 3-10. The oscillatory pressure and microwave Doppler shift components were band-pass filtered at the oscillatory pressure driver frequency. Data acquisition and processing were as described in Ref. 4.

3.3.2 Results

Real and imaginary parts of the combustion response function versus frequency, for the LS-87 (coarse AP) propellant are shown in Figure 3-11. The data points are the median of the several data reductions carried out over the interval of individual tests. The clearly established zero in the imaginary part at about 650 Hz establishes a peak in the real part at about that frequency. The nature of the real part data would also support a peak there. The valley at about 720 Hz may not be as pronounced as indicated, being defined by only one datum point. The appearance of a second peak at about 1200 Hz is supported by both the trend in the real part data and by the approach to a second zero in the imaginary part data. Moving toward lower frequencies, as the frequency approaches zero the real part appears to be approaching the pressure exponent and the imaginary part is approaching zero - credible results.

Figure 3-12a is a composite plot of the response functions for the three propellants tested. They are similar in character, with similar magnitudes and locations of peak response frequencies. This was surprising in view of the disparities in AP particle size for the three propellants. Smoothing out the apparent valley for the coarse propellant would make the three curves look even more alike. On the other hand, this similarity is not inconsistent with the similarity in the constant-pressure mean and dynamic burning data discussed previously.

For comparative purposes, data for three Hercules ABL propellants acquired with a predecessor microwave apparatus on another program (Ref. 20) are shown in Figure 3-12b. These propellants contain 87% AP in HTPB binder, with particle sizes as indicated on the figure. The peak responses are occurring at lower frequencies in this group, but within the group the peak response frequencies are not strongly sensitive to particle size. However, the response function magnitudes are significantly affected by particle size.

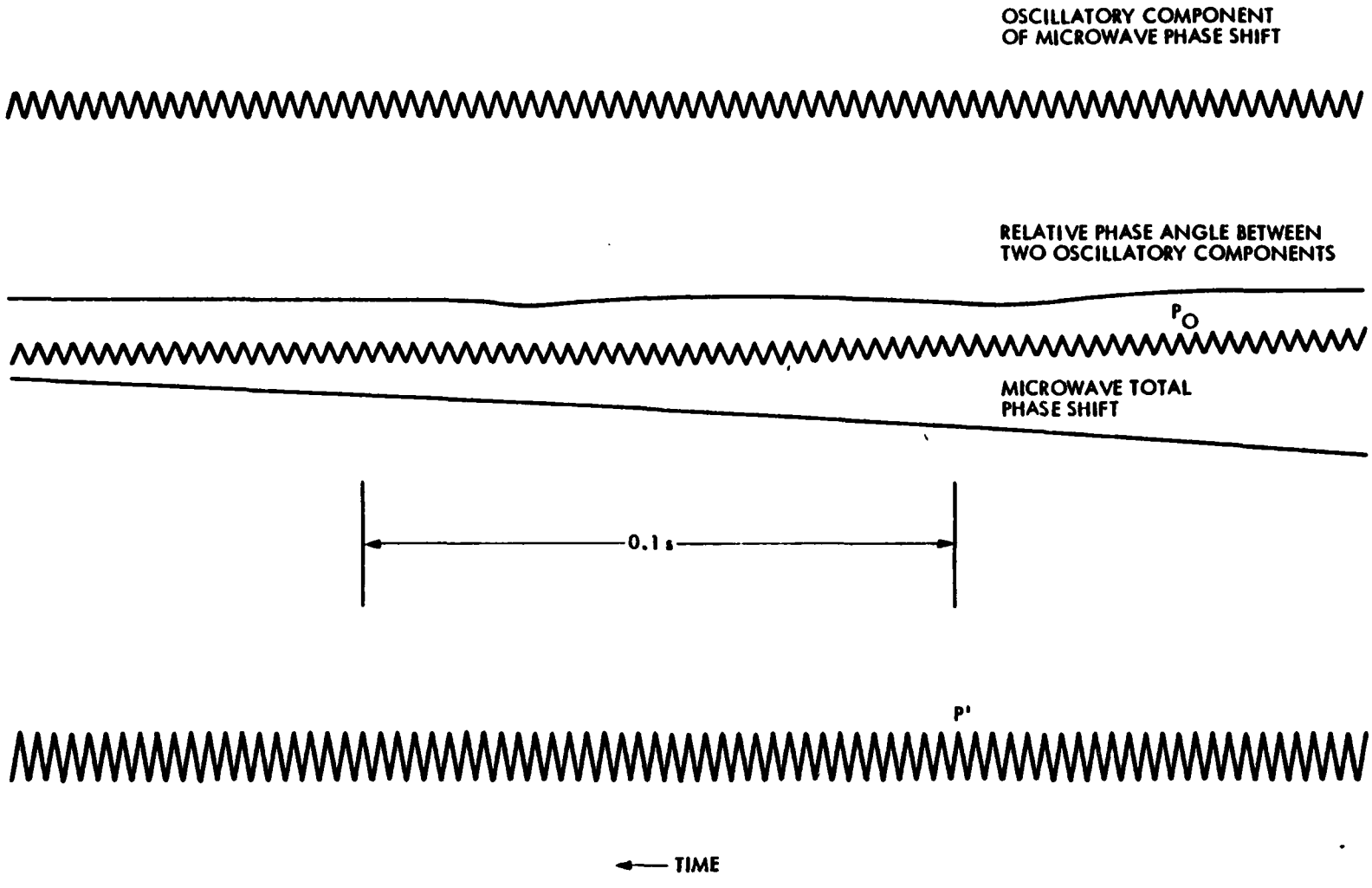

Figure 3-10. Portion of Test Record of Dynamic Burning Rate Data Under Imposed Oscillatory Pressure Conditions - LS-87 Propellants 350 Mz, 3.5 MPa Mean Pressure

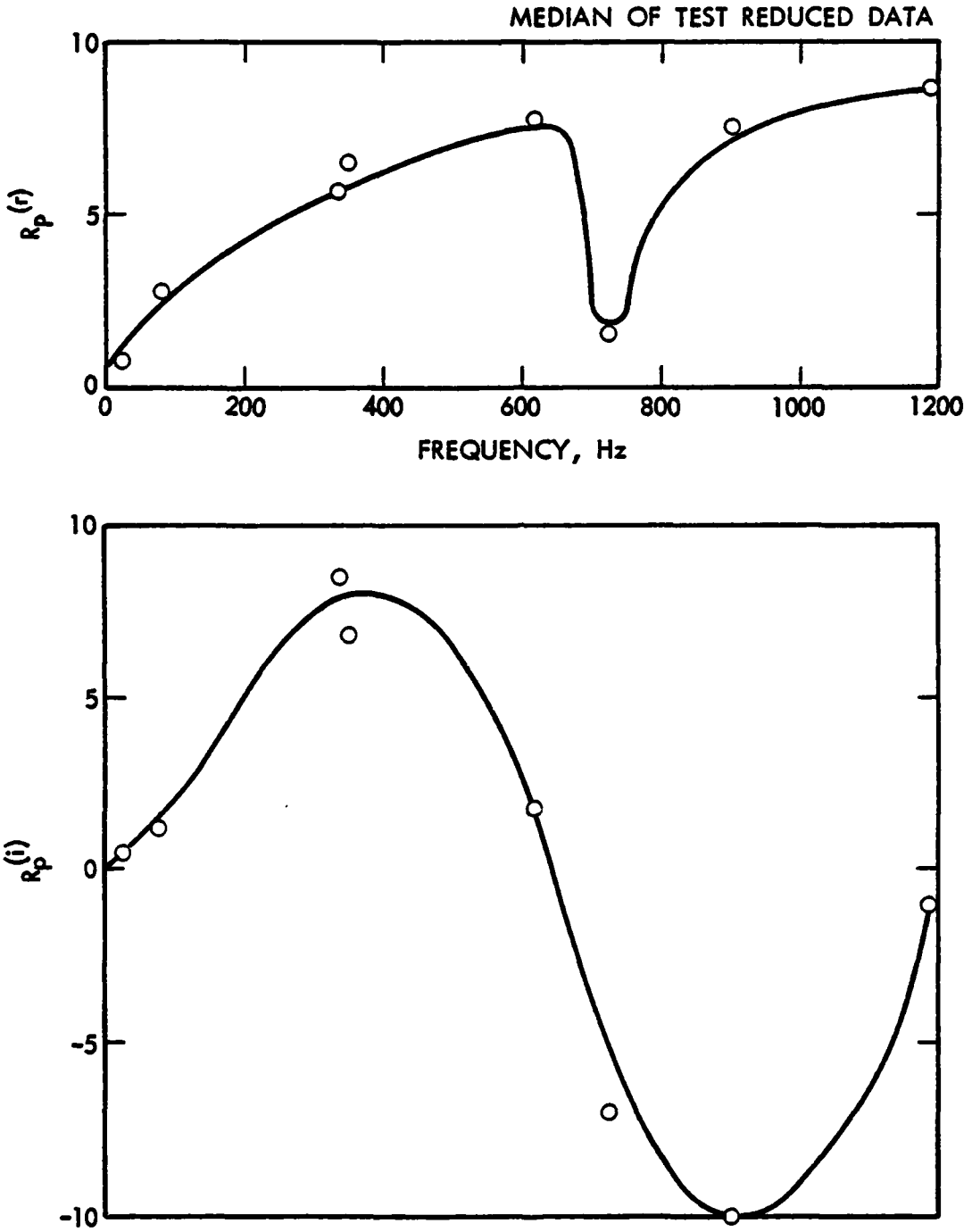

Figure 3-11. Measured Real and Imaginary Parts of the Response Function Versus Frequency for the LS-87 Propellant

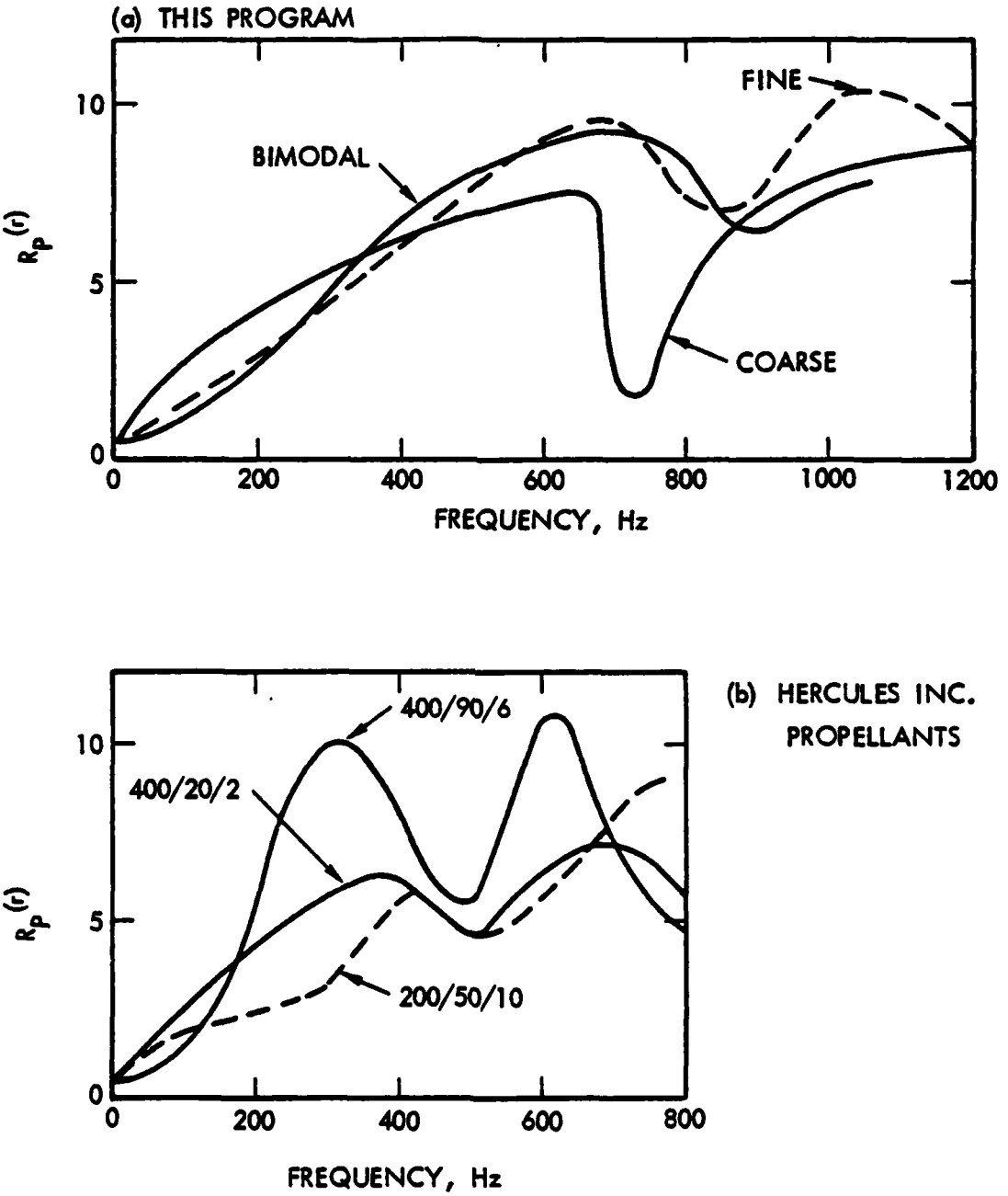

Figure 3-12. Response Function Real Part Versus Frequency Curves for Two Sets of Propellants, 3.5 MPa

Table 3-5 attempts to put all of the data together by listing characteristic dimensions associated with the peak response frequencies. In the case of the JPL propellants studied in this program, the characteristic dimensions are roughly the same. In the case of the Hercules propellents as a group, they are also roughly the same, but take on different values from the JPL propellants. The characteristic dimensions for the JPL propellants cannot be correlated with the EDAX/SEM data, but can be associated with two of the characteristic dimensions appearing in the dynamic burning data (Table 3-3). It is not clear why these particular dimensions would be preferred; they are not correlatable with the size distributions. Some other explanation must be sought for these characteristic dimensions, their apparent constancy within each group of propellants and their difference between the two groups of propellants.

These experimental results do not validate the proposed theoretical method for predicting effects of heterogeneity on the combustion response of composite propellants. Peak response frequencies cannot be simply correlated with AP particle size distribution. Characteristic dimensions which can be associated with these frequencies are not amenable to a priori identification from the propellant microstructure or dynamic burning at constant pressure. On the other hand, the results contribute to a growing data bank which invalidates the classical theory because of the multiple peaks and multiple zero phases. Data for homogeneous (e.g., double-base) propellants would be interesting for comparative purposes, to see whether or not such multiples appear. The compositional response aspect of the proposed theory may still be a valid basis to explain effects of heterogeneity, but may require a process other than inherent microstructure for its implementation.

Table 3-5. Comparison of Peak Response Characteristic Dimensions and Size Distributions

Propellant Designation	Mean Sizes in AP Distribution	Burn Rate at 3.5 MPa	Characteristic Dimensions Associated with Peak Response Frequencies
LS-87	200 μm	0.51 cm/sec	8 μm
			4
LS-88	10	0.53	8
			5
LS-89	200	0.43	7
	10		4
SD-868	200	0.90	
	50		21
	10		12
SD-870	400	0.68	
	20		18
	2		10
SD-872	400	0.70	
	90		22
	6		11

SECTION 4

TECHNICAL PUBLICATIONS

4.1 AIAA PUBLICATIONS

The following papers were published by journals of the American Institute of Aeronautics and Astronautics in the course of this research program. These papers cover work done in the most recent of the prior research programs as well as work done under the current program.

(1) Cohen, N. S., and Strand, L. D., "Analytical Model of High Pressure Burning Rates in a Transient Environment" AIAA J., Vol. 18, No. 8, August 1980, pp. 968-972.

(2) Strand, L. D., and Cohen, N. S., "Effect of HMX on the Combustion Response Function," J. Spacecraft and Rockets, Vol. 17, No. 6, November-December 1980, pp. 566-568.

(3) Cohen, N. S., "Response Function Theories That Account for Size Distribution Effects - A Review," AIAA J., Vol. 19, No. 7, July 1981, pp. 907-912.

(4) Strand, L. D., and Cohen, N. S., "Porous Plate Analog Burner Study of Composite Solid Propellant Flame Structure," AIAA J., Vol. 20, No. 4, April 1982, pp. 569-570.

(5) Cohen, N. S., and Strand, L. D., "An Improved Model for the Combustion of AP Composite Propellants," AIAA J., Vol. 20, No. 12, December 1982, pp. 1739-1746.

(6) Cohen, N. S., "A Pocket Model for Aluminum Agglomeration in Composite Propellants," AIAA J., Vol. 21, No. 5, May 1983, pp. 720-725.

In addition, the following two papers have been submitted for AIAA Journal publication. The first has been accepted with revisions, the second is in review.

(7) Cohen, N. S., and Strand, L. D., "Combustion Response to Compositional Fluctuations," presented as AIAA Paper 83-0476, AIAA 21st Aerospace Sciences Meeting, Reno, Nevada, January 1983.

(8) Cohen, N. S., and Strand. L. D., "Effects of AP Particle Size on Combustion Response to Crossflow," presented as AIAA Paper 83-1270, AIAA/SAE/ASME 19th Joint Propulsion Conference, Seattle, Washington, June 1983.

It is planned to present and publish a paper on the most recent work of the current program in the near future. It will probably appear as

(9) Strand, L. D., and Cohen, N. S., "Relation Between Composite Propellant Heterogeneity and Nonsteady Burning."

Finally, it is planned to prepare a technical note which will probably appear as

(10) Cohen, N. S., and Strand, L. D., "Applicability of Classical Combustion Response Theory to Nitramine Propellants."

4.2 ANNUAL RESEARCH PROGRESS REPORTS

Research Progress during the previous two annual increments were summarized in the following Annual Research Progress Reports.

(1) Cohen, N. S., and Strand, L. D. "Non-Steady Combustion of Composite Solid Propellants," publication 7000-7, Jet Propulsion Laboratory/California Institute of Technology, Pasadena, California, April 1982.

(2) Cohen, N. S., and Strand, L. D., "Non-Steady Combustion of Composite Solid Propellants," publication JPL-D-708, Jet Propulsion Laboratory/California Institute of Technology, Pasadena, California, May 1983.

4.3 OTHER

Presentations were given at each the 17th and 18th JANNAF Combustion Meetings, and the associated papers were published in the proceedings of those meetings.

Presentations were also made at the 1981, 1982 and 1983 AFOSR/AFRPL Rocket Propulsion Research Meetings. Abstracts were published in the Book of Abstracts for each of these meetings. In addition, an abstract was submitted for the 1984 meeting.

A dissertation detailing the analytical modeling of combustion response to heterogeneity was prepared and informally distributed to the Air Force Program Manager and to interested colleagues. Finally, a summary paper dealing with the status of combustion instability research and technology was prepared and informally distributed to the Air Force Program Manager.

SECTION 5

PROFESSIONAL PERSONNEL

The Principal Investigator for this program was Mr. Leon D. Strand of the Propulsion Systems Section (M/S 125-224), Jet Propulsion Laboratory/ California Institute of Technology, 4800 Oak Grove Drive, Pasadena, CA 91109 (telephone 818-354-3108). His co-investigator was Dr. Norman S. Cohen, Cohen Professional Services, 141 Channing Street, Redlands, CA 92373 (telephone 714-792-8807). Mr. Strand was responsible for the overall program and specifically responsible for the experimental work performed. Dr. Cohen worked on this program under subcontract, and was responsible for the analytical modeling.

SECTION 6

CONCLUSIONS AND RECOMMENDATIONS

Assuming that compositional fluctuations occur in the course of burning of composite propellants, the combustion response to such fluctuations is a relatively strong response compared to the response to pressure perturbations. In this context, the dependence of burning rate on AP concentration becomes an important combustion parameter. Combustion model calculations are in good agreement with data for that parameter; it tends to be an order of magnitude larger than pressure exponent. If compositional fluctuations occur in the course of pressure oscillations at the same frequency, the overall combustion response will be augmented significantly. This could remedy deficiencies in the classical combustion response theory as applied to composite propellants.

The combustion response to velocity fluctuations can be comparable to the compositional response, and therefore also larger than the response to pressure perturbations. Combustion model calculations and data are in agreement and support a "velocity exponent" larger than pressure exponent. Compositional fluctuations would augment velocity-coupled response, but is not as potentially dominant as in the case of pressure-coupled response.

Parametric studies with the combustion models show, as a general trend, that the several components of combustion response tend to increase with increasing AP particle size and pressure. These variations in particle size and pressure promote AP flame control of the combustion. It is a more responsive (less stable) form of flame because it is of lower energy and kinetically-limited. Diffusion flame control tends to promote stability.

Parametric studies also show that combustion response tends to increase with decreasing mean flow velocity, in particular the response to velocity fluctuations. Effects of AP particle size, pressure and mean flow velocity on the velocity-coupled response can be correlated with data on nonlinear combustion instability.

Measured periodicities in the microstructures of composite propellants are more systematic than one would expect from the distributions of particle sizes and shapes in real propellants, but are much less systematic than exists in an idealized packed bed of unimodel spheres. Compositional fluctuations derived from these data have amplitudes of about $\pm$ 5% of the nominal AP concentration. The frequency distributions can be associated with the particle size distributions of the propellants.

There are burning rate fluctuations in composite propellants burning at constant pressure. The frequency distributions are broad-banded and repeatable, but do not correlate with particle size distribution. For the propellants tested, the frequency distribution appeared to be independent of the size distribution. The amplitudes of the burning rate fluctuations were roughly 20% of the mean burning rate. Thus the measured compositional response

is roughly 4, a reasonable value in the light of model calculations and measured dependencies of burn rate on AP content. Data should be obtained for homogeneous (double-base) propellants, where compositional fluctuations and such dynamic burning would not be expected.

For the propellants tested, pressure-coupled response function versus frequency curves were not strongly affected by AP size distribution. The propellants exhibited 2 peaks in the real parts of the combustion response, supported by measured zeroes in the imaginary parts. The peak response frequencies were comparable for these propellants, such that associated microstructure characteristic dimensions were about the same. Thus the inherent microstructure periodicities are not the source of compositional fluctuations affecting the combustion response.

Another series of 3 propellants also showed 2 peaks in the real parts, and also had associated characteristic dimensions that were about the same in spite of significant differences in AP size distribution. However, these dimensions differed from the dimensions of the first group, and the magnitudes of the response showed a greater dependence on size distribution. Thus there are size distribution effects, but their origins have not been established. Future work should include combustion response measurements for homogeneous propellants, where heterogeneity effects should be absent.

Mechanistic investigations and associated analytical modeling should seek some other process that would give rise to compositional fluctuations in the combustion of composite propellants. One possibility is a different response in the regressions of AP and binder. Effects of particle size would then appear through their effects on combustion as a function of oxidizer/fuel ratio, rather than through microstructure periodicities.

SECTION 7

REFERENCES

1. Cohen, N. S., "Response Function Theories That Account for Size Distribution Effects - A. Review," AIAA J., Vol. 19, No. 7, July 1981, pp. 907-912.

2. Cohen, N. S., and Strand, L. D., "Combustion Response to Compositional Fluctuations," AIAA Paper 83-0476, 21st AIAA Aerospace Sciences Meeting, Jan. 1983.

3. Cohen, N. S., and Strand, L. D., "Effects of AP Particle Size on Combustion Response to Crossflow," AIAA Paper 83-1270, AIAA/SAE/ASME 19th Joint Propulsion Conference, June 1983.

4. Strand, L. D., Magiawala, K. R., and McNamara, R. P., "Microwave Measurement of the Solid Propellant Pressure-Coupled Response Function," J. Spacecraft and Rockets, Vol. 17, Dec. 1980, pp. 483-488.

5. Cohen, N. S., and Strand, L. D., "Analytical Model of Contributions of Composite Propellant Heterogeneity to the Combustion Response Function," supplemental dissertation prepared and submitted under AFOSR-ISSA-81-0019, Jet Propulsion Laboratory/California Institute of Technology, Pasadena, CA, March 1982.

6. Cohen, N. S., and Strand, L. D., "An Improved Model for the Combustion of AP Composite Propellants," AIAA Journal, Vol. 20, No. 12, Dec. 1982, pp 1739-1746.

7. Saderholm, C. A., "A Characterization of Erosive Burning for Composite H-Series Propellants," AIAA Solid Propellant Rocket Conference, Palo Alto, CA, Jan. 1964.

8. King, M. K., "A Model of the Effects of Pressure and Crossflow Velocity on Composite Propellant Burning Rate," AIAA Paper 79-1171, AIAA/SAE/ASME 15th Joint Propulsion Conference, June 1979.

9. Culick, F. E. C., "Calculation of the Admittance Function for a Burning Surface," Astronautic Acta, Vol. 13, 1967, pp. 221-237.

10. Levine, J. N., and Baum, J. D., "A Numerical Study of Nonlinear Instability Phenomena in Solid Rocket Motors, AIAA Paper 81-1524, AIAA/SAE/ASME 17th Joint Propulsion Conference, July 1981.

11. Powell, E. A., Padmanabhan, M. S., and Zinn, B. T., "Approximate Nonlinear Analysis of Solid Rocket Motors and T-Burners," AFRPL-TR-77-48, Georgia Institute of Technology, Atlanta, GA, July 1977.

12. Culick, F. E. C., "Nonliner Behavior of Acoustic Waves in Combustion Chambers," Acta Astronautica, Vol. 3, 1976, pp. 715-757.

13. Flandro, G., "Nonlinear Transient Combustion of a Solid Rocket Propellant," AIAA Paper 83-1269, AIAA/SAE/ASME 19th Joint Propulsion Conference, July 1983.

14. Brownlee, W. G., "Nonlinear Axial Combustion Instability in Solid Propellant Rocket Motors," AIAA Journal, Vol. 2, No. 2, Feb. 1964, pp. 275-284.

15. Roberts, A. K., and Brownlee, W. G., "Nonlinear Longitudinal Combustion Instability: Influence of Propellant Composition," AIAA Journal, Vol. 9, No. 1, Jan. 1971, pp. 140-146.

16. Hughes, P. M., and Smith, D. L., "Nonlinear Combustion Instability in Solid Propellant Rocket Motors - Influence of Geometry and Propellant Formulation," 53rd Meeting of the Propulsion and Energetics Panel of AGARD, AGARD-CP-259 on Solid Rocket Motor Technology, Paper No. 26, April 1979.

17. Kooker, D. E., and Nelson, C. W., "Numerical Solution of Three Solid Propellant Combustion Models During a Pressure Transient," BRL-R-1953, U.S. Army Ballistics Research Laboratories, Aberdeen Proving Ground, MD, Jan. 1977.

18. Tien, J. S., "Oscillatory Burning of Solid Propellants Including Gas Phase Time Lag," J. Combustion Science and Technology, Vol. 5, 1972, pp. 47-54.

19. Rudy, T. P. and Bain, L. S., "Chemical Control of Propellant Properties," AFRPL-TR-81-53, Chemical Systems Division of United Technologies, Sunnyvale, CA, Aug. 1981.

20. Strand, L. D., "Investigation of Microwave Doppler Shift Measurement of Solid Propellant Combustion Response Function," AFRPL-TR-83-085, Jet Propulsion Laboratory, Pasadena, CA, Jan. 1984.

END

FILMED

4-85

DTIC